UNITED STATES DEPARTMENT OF THE INTERIOR
GEOLOGICAL SURVEY

An Alternative Hypothesis for Sink Development Above Salt Cavities in the Detroit Area

By

Daniel Stump, A. S. Nieto,
and John R. Ege.

Open-File Report 82-297

1982

CONTENTS

ILLUSTRATIONS

ILLUSTRATIONS--Continued

TABLES

An Alternative Hypothesis for Sink Development Above Salt Cavities in the Detroit Area

By
Daniel Stump, A. S. Nieto[1],
and John R. Ege

ABSTRACT

Subsidence and sink formation resulting from brining operations in the Windsor-Detroit area include the 1954 sink at the Canadian Salt Company brine field near Windsor, Ontario, and the 1971 sinks at the BASF Wyandotte Corporation brine field at Grosse Ile, Mich. Earlier investigations into both occurrences concluded that the mechanism of sink development consisted of the gradual stoping of poorly supported brine-gallery roof rock to the near surface with subsequent surface collapse. A more recent study attempted to describe the mechanism of sink development in terms of the geometry of a cylindrical chimney formed by stoping of roof rock, the height of a cavity at depth, the depth of overlying rock, and the bulking ratio of the rubble formed during stoping.

Persons with extensive experience in solution mining in the Windsor-Detroit area have expressed doubt that the stoping mechanism could fully explain the development of these sinks. Further, they have proposed that the relatively shallow (300-ft-deep) Sylvania Sandstone, in this case, may be responsible for the sinks by a secondary undermining mechanism to be examined in this paper. The mechanism involves downwarping of the beds overlying the salt cavity and development of a shallower cavity in the Sylvania Sandstone by downward migration of cohesionless sand grains from the Sylvania through openings in the disturbed rock to the lower cavity. This study indicates that under natural conditions the Sylvania will not migrate, even in the presence of large underground water flows because the sandstone possesses some cohesion throughout its depth. However, further investigation has formulated a mechanism that could allow the Sylvania Sandstone to loose its cohesion in response to high horizontal stresses. These stresses could be the result of deformation that accompanies general subsidence and (or) of past geologic processes.

---

[1]University of Illinois, Champaign, Illinois 61820

Included in this study were experimental and analytical investigations. As determined by uniaxial and triaxial testing, the Sylvania Sandstone in the Detroit area has been shown to have low compressive strength. In addition, it exhibits an explosive type failure whereby over 50 percent of the sample is reduced to loose granular sand. As a result of these characteristics, the Sylvania Sandstone can loose its cohesion when subjected to high horizontal stresses.

Efforts at mechanically modeling the Sylvania were made to account for the measurements and observations. Linear arch theory was used for an elastic analysis. Linear arch theory predicts two modes of failure: (1) arch crushing, a compressive failure of the upper portion of the arch due to compressive stresses exceeding the compressive strength of the material, and (2) arch collapse, a sagging of the beds due to compressive strains which reduce the arch line to a length less than the original arch length. The arch crushing mode of failure would then yield the loose granular sand as observed in laboratory testing. Arch collapse would simply result in bed sagging without granulation of the sandstone. Arch collapse is favored by thin-bedded material while arch crushing is favored by thick-bedded material. Arch crushing seems to be a likely mode of failure for the Windsor-Detroit sinks.

It is believed that after a crushing failure the sand-water slurry (specific gravity 1.2) which exceeds the density of the cavity brine will migrate downward through cracks and open joints eventually reaching the practically limitless open spaces of the rubble column and salt cavity. As the extent of the cavity within the Sylvania increases in depth and width because of sand migration, a critical span will be reached where the immediately overlying upper Sylvania and the overlying Detroit River Dolomite will fail. The collapse will allow a path for the approximately 100 ft of clay to collapse, resulting in a sink as the surface manifestation.

INTRODUCTION

The U.S. Geological Survey is conducting earth-science research into the occurrences and mechanisms of land subsidence which can be described as a local mass sinking of the ground surface. One current activity in geologic research, the Solution Subsidence and Collapse project, deals with ground subsidence over underground openings formed by both natural and artificial dissolution of soluble rocks such as salt and limestone (Ege, 1979a, 1979b, 1979c; Savage, 1979). The research effort is intended to identify and improve our understanding of geologic processes that may be hazardous to life and property and to determine geographic distribution and expected frequency and severity of these processes.

This report summarizes a geological and geomechanical study made of subsidence and sink formations in the Detroit area as a result of salt solution mining. The research was a cooperative effort between the U.S. Geological Survey, University of Illinois, Solution Mining Research Institute, and BASF Wyandotte Corporation.

The basic method of solution mining consists of drilling holes to the salt or evaporite deposit, injecting fresh water or undersaturated brine down the well in order to dissolve the soluble minerals, and then removing the resulting brine. A fluid-filled void is consequently formed in the region formerly occupied by the salt or evaporite beds (Querio, 1977). A similar process can occur in nature only if geologic conditions are such that a source flow of water is in contact with an evaporite deposit so that soluble minerals in the deposit can go into solution and then be removed. Under the proper conditions surface brines, salt caves, and collapse features will form (Landes, 1963).

Subsidence and sink formation, as a result of brining operations in the Windsor-Detroit area, include the 1954 sink that occurred at the Canadian Salt brine field near Windsor, Ontario, and the 1971 sinks at the BASF Wyandotte Corporation brine field at Grosse Ile, Michigan. Initial investigations following both occurrences concluded that the mechanism of sink development consisted of the gradual stoping of poorly supported brine-gallery roof rock to the near surface with subsequent surface collapse (R. B. Peck, written commun., 1954). A later study (Nieto-Pescetto and Hendron, 1977) defined the mechanism of sink development in terms of the geometry of a cylindrical chimney formed by stoping of roof rock, the thickness of the cavity at depth, the depth of overlying rock, and the bulking ratio of the rubble formed during stoping.

Persons with experience in solution mining in the Windsor-Detroit area (A. J. Robinson and T. B. Piper, oral commun., 1978) expressed doubt that the stoping mechanism could fully explain the development of sinks. Further, they have suggested that a granular material such as the relatively shallow (300-ft deep) Sylvania Sandstone (fig. 1) may be directly responsible for the sinks. It has been speculated that broken casings adjacent to the Sylvania could induce water flows that would enable the "loose" Sylvania Sandstone to form a slurry of sufficient density to allow it to be washed down cracks or joints or in rock layers or abandoned well casings. This activity would create a new, shallower cavity within the Sylvania Sandstone that would eventually result in a surface sink. Spalling and large water inflows during shaft excavation, and the spontaneous loss of cohesion of Sylvania cores with time have been cited as further evidence of the "loose" nature of the Sylvania Sandstone.

The main effort of the present study was to critically examine the proposed alternative mechanism and the role of the Sylvania Sandstone in sink development in the Detroit area. Although not entirely as originally proposed, the Sylvania seems to play an important role in sink development. This study indicates according to local brinefield operators, that under normal conditions the Sylvania will not flow, even in the presence of large water flows from broken casings because the sandstone possesses some cohesion throughout its depth. However, a mechanism is proposed that could allow the Sylvania Sandstone to fail in compression and loose its cohesion if subjected

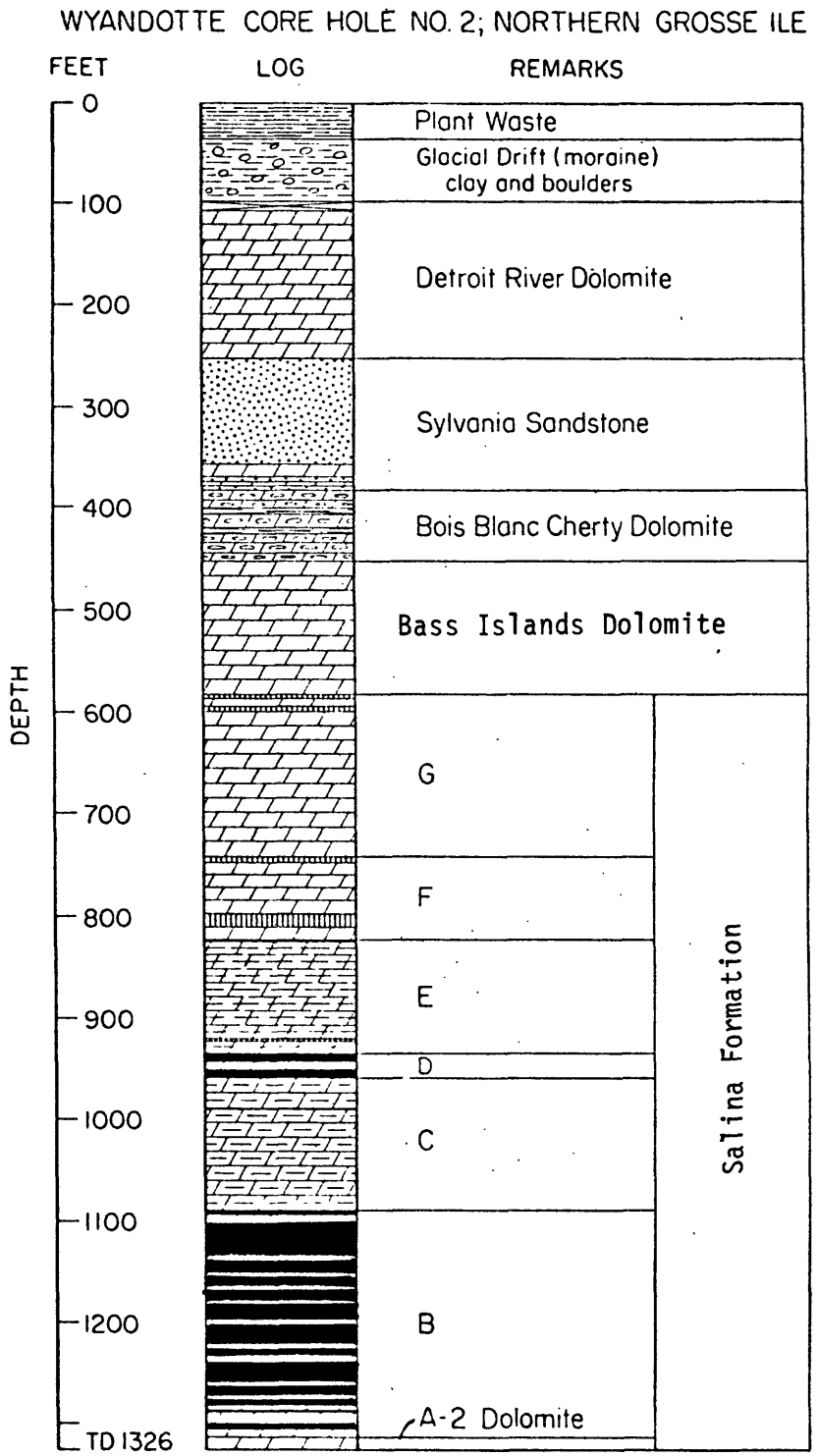

Figure 1.--Typical core log of Point Hennepin brine field. Solid pattern shows salt beds, vertical lines designate anhydrite layers, rhombic bricks are dolomite, and the flattened circles represent chert nodules. Unit E is dolomitic shale and unit C is shaly dolomite; both contain some anhydrite and salt (after Landes and Piper, 1972).

to high horizontal stresses. These high horizontal stresses could be the result of deformation that accompanies general trough subsidence, and of past geologic processes. In this context, high flows of water from broken casings are seen as triggering compressive failure in the Sylvania Sandstone by a reduction in effective stresses, and perhaps initiating the downward flow of the failed, cohesionless sand.

PREVIOUS WORK

The early engineering-geological reports of the area were concerned with general subsidence as a consequence of salt removal at depth (800-1,000 ft) through brine wells, and its effect on buildings and other structures overlying the North Works brine field (operated by the former Wyandotte Chemicals Corporation) at Wyandotte, Michigan. (fig. 2). These reports attributed the subsidence to downwarping of brine well cavity roof rock (R. B. Peck, written commun., 1946; Karl Terzaghi, written commun., 1948). Terzaghi considered the rock strata overlying the solution cavities as a thick plate; he postulated that every plate or beam which spans an open space sags under the influence of its own weight. Sagging would be initiated by removal of support from salt cavity development and induce tensile failure in the immediate brine-cavity roof rock and the falling of this material to the base of the brine cavity. The stoping of the roof rock would reduce the thickness of the beam or plate; hence stoping would cause increasing sag and, in turn, surface subsidence. Terzaghi also discussed the geometrical relationships of stoping in various rock materials which bulked at different rates.

A detailed report reviewing all aspects previously published on subsidence was consequently published (Karl Terzaghi and others, written commun., 1950) This report included data concerning brine cavity geometry, at the BASF North and South works, level monument reference points, and grid patterns and included excellent sketches of the stoping mechanism as visualized at that time and details of subsidences in other areas of the world. This report was the culmination of subsidence investigation concerning the mainland (North and South Works) brine field operation. The potential of damage to buildings and structures prompted relocating the brine operation to Point Hennepin on Grosse Ile, Mich. (fig. 2) in the late 1940's and early 1950's.

In 1954 a sink unrelated to the above subsidence formed in the brine fields of the Canadian Salt Company and Canadian Industries, Ltd., at Windsor, Ontario (T. B. Piper, written commun.,1954; R. B. Peck and Karl Terzaghi, written commun., 1954). This event was of considerable practical and academic value as records of systematic surface elevation observations taken prior to development of the sink were available. Karl Terzaghi (1954) observed that the events preceding the sink formation at Windsor corresponded with other similar events he had observed in Europe. In brief, his observed sequence of events is as follows:

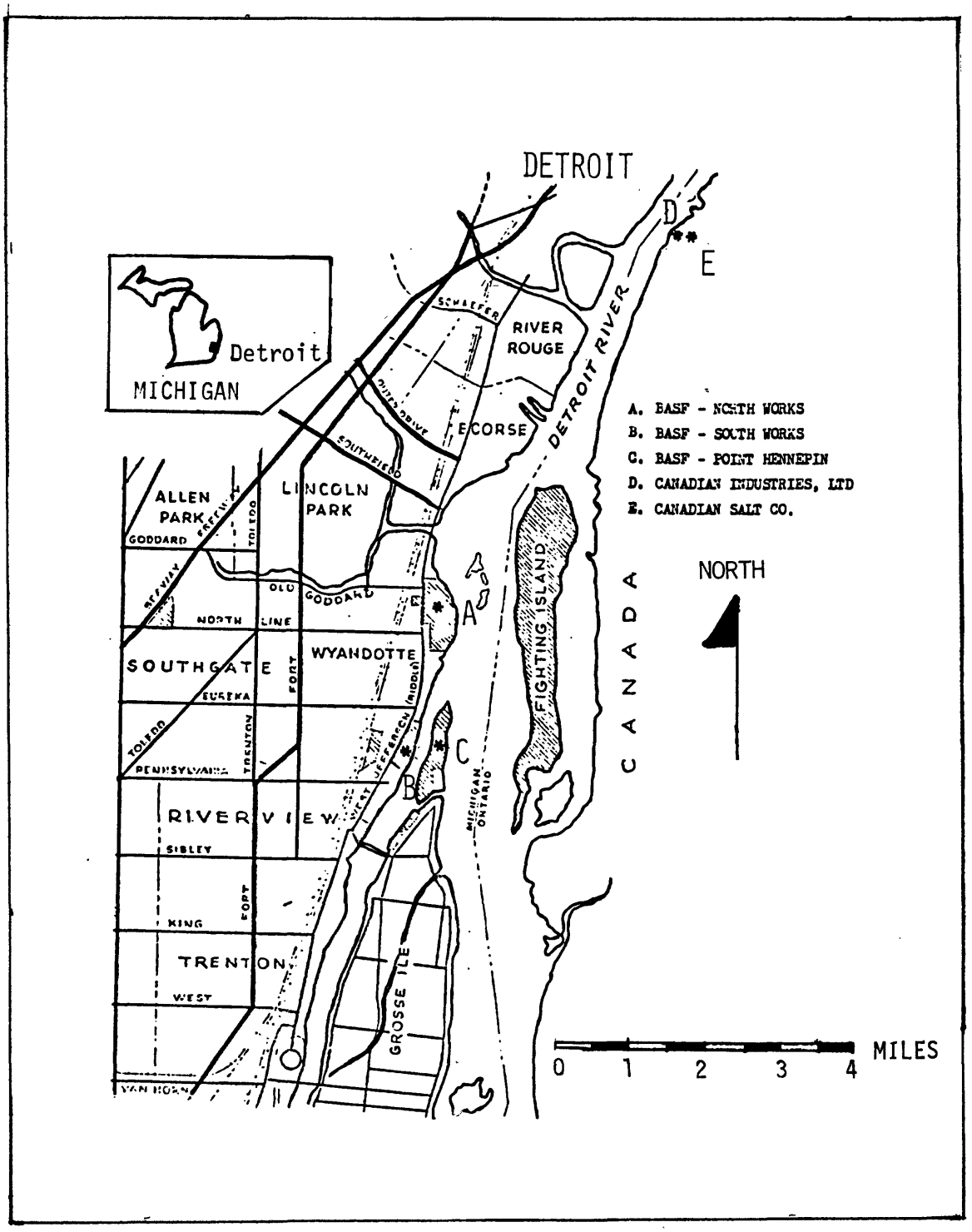

Figure 2.--Map showing location of various operator brine fields (in the Detroit area) of concern to this paper.

1. General regional subsidence at slow rates over many years,
2. Indication of areal topographic changes, i.e. tension cracks in buildings and (or) foundations, breaking of pipelines,
3. Acceleration of subsidence a few years prior to sink development,
4. A sink of approximately 100 ft in diameter indicating a cylindrical chimney of stoping.
5. Termination of activity.

Further, Terzaghi observed that sinks usually occur in families, although only one was observed at Windsor, Ontario.

General subsidence manifested itself again in the middle 1950's at the Point Hennepin brine field on Grosse Ile, Mich. The brining operation caused coalescing of individual brine wells into larger galleries and the two bowls of subsidence formed over two such salt-well galleries. Recommendations were given (R. B. Peck, written commun., 1959) to create separate galleries of limited size in order to minimize subsidence. New operation methods were also recommended which were enacted.

Despite the initiation of new operation methods the Point Hennepin brine field experienced increased rates of subsidence and the North Gallery developed a sink on January 9, 1971. On April 28, 1971, collapsing began above the Central Gallery (one-half mile south of the North Gallery); this sink subsequently developed a satellite (fig. 3) as (Karl Terzaghi, written commun., 1954) had been observed in other parts of the world.

Production was discontinued at the North and Central Galleries. The brine field was relocated to the southern extremes of Point Hennepin. In the fall and winter of 1975 precise level measurements revealed increasing rates of subsidence in an area of the Southwest Gallery on Point Hennepin. This prompted the operator to investigate the subsidence with a drilling program. Test drilling revealed a 6-ft cavity (Dowhan, 1976) in the Sylvania Sandstone approximately 30 ft from the top of the sandstone. The drilling revealed zones of broken dolomite and (or) lost circulation from 770 to 931 ft. A sonar survey made of the void within the Sylvania Sandstone indicated that the open zone (first sonar reflection) extended 280-300 ft in a north and northeasterly direction, 70 ft to the east and west and 10 ft to the south.

A study conducted after the Point Hennepin sinks (Nieto-Pescetto and Hendron, 1977) attempted to define the mechanism of sink development in terms of the geometry of a cylindrical chimney formed by stoping of roof rock, the thickness of the cavity at depth, the depth of overlying rock and the bulking ratio of the rubble formed during stoping. Critical rock surface slopes in the subsidence bowl were identified as indicators of imminent sink development. However, the above-mentioned mechanism can be questioned on several grounds (Nieto, 1979). First, volume relations require that the entire B-salt unit be completely dissolved. However, exploratory drilling just before collapse indicated that the B-salt was intact. Second, sinks are

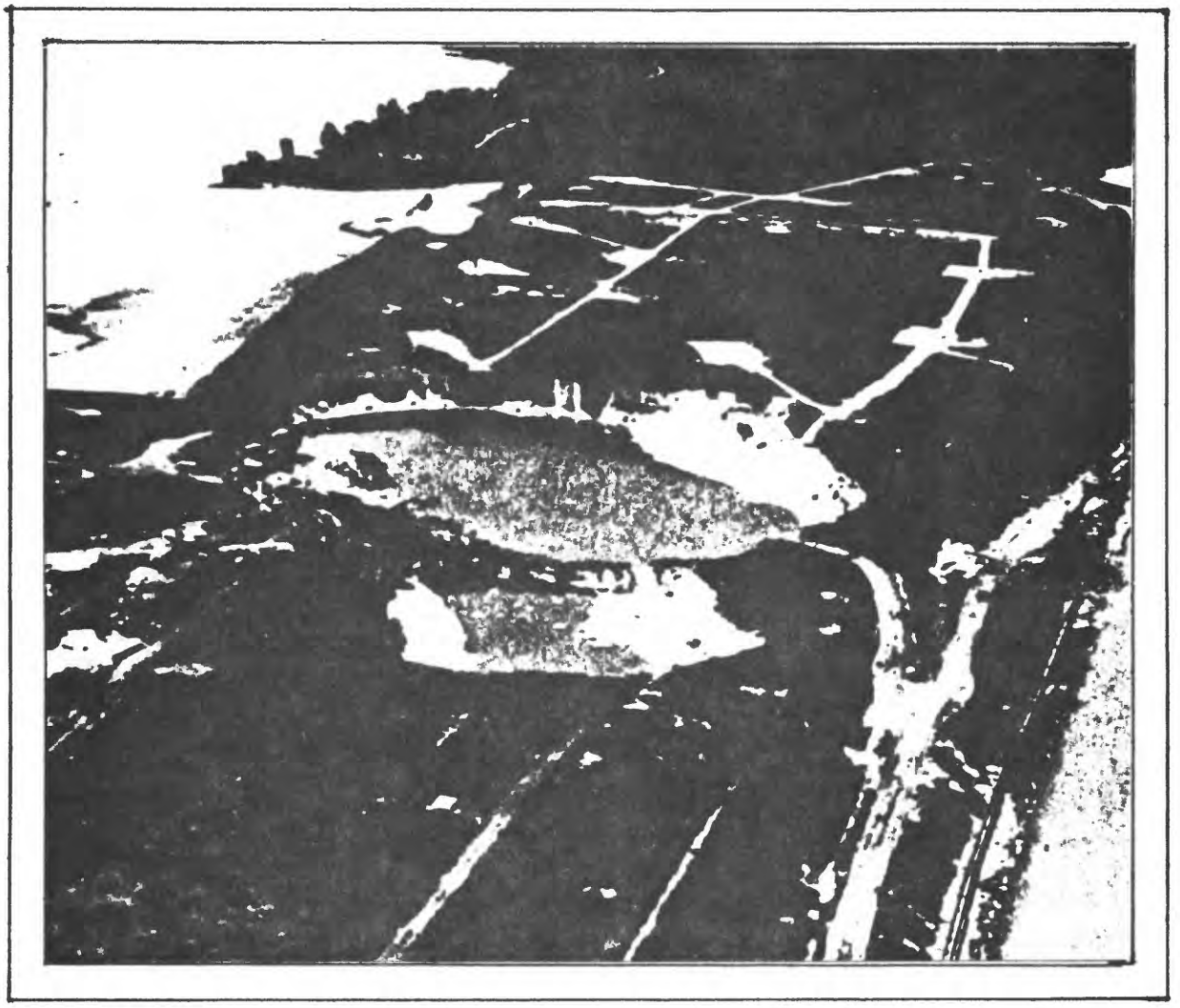

Figure 3.--View of Center Gallery sink looking south. Roadways and well sites of active (background) and abandoned (foreground) wells can be seen on the upper level of the retired waste bed. Water level in crater stands at river level. Waste material is semiplastic, moist and chalky in character developing vertical cliffs where undermined. Satellite hole adjacent to center gallery sink appears to be shallower, is included in line of zero cracks which encircles craters and includes broken ground northeast of main crater (after Landes and Piper, 1972).

found in the Illinois Basin in flat-lying layered rock where ratios of mined material to overburden is 1:5 or greater. At Point Hennepin and Windsor, Ontario, the ratios are much smaller (one-tenth to one-fifteenth). Third, the mechanism uses bulk ratios shown to be too small by down hole photographs of the rubble. None of these objections taken separately will negate the hypothesis, but taken together cast doubt on the viability of the mechanism.

The present effort is directed to defining an alternative mechanism of sink formation in accordance with data available from Windsor and Point Hennepin as examples.

GENERAL GEOLOGIC SETTING

Stratigraphy and Lithology

Overburden above bedrock in the Detroit area consists of approximately 60-80 ft of Pleistocene age deposits of lacustrine clays overlying bedrock boulders locally referred to as glacial till. At the Point Hennepin brine field, approximately 30 ft of insoluble plant waste solids have been deposited on the normal Pleistocene deposits (fig. 1) in a tailings pond activity prior to salt-well operations.

In the subsurface rock units consist of sedimentary deposits of Devonian, Silurian, Ordovician and Cambrian age resting on Precambrian basement rocks. The sedimentary section underlying the Point Hennepin brine field consist of mostly dolomite and sandstone. The Middle Devonian strata consists of the Detroit River Dolomite; the Sylvania Sandstone and the Lower Devonian strata consist of the Bois Blanc Formation. The Detroit River Dolomite is approximately 145 ft thick. The Sylvania Sandstone below the Detroit River Dolomite is approximately 125 ft thick. The Lower Devonian unit is the Bois Blanc Formation of approximately 85 ft in thickness.

At Grosse Ile Upper Silurian strata present consist of the Bass Islands Dolomite and the Salina Formation. The Bass Islands Dolomite is approximately 160 ft thick. The Salina Formation is approximately 800 ft thick and has been subdivided into units G (youngest) to A (Landes, 1945). Major salt beds exploited by brine field operators in the Detoit area have been from within the Salina F (locally 150 ft thick), D and B (240 ft thick) units. Presently, the Point Hennepin brine field operator has restricted exploitation to the Salina B unit. The remaining units of the stratigraphic column (Dorr and Eschman, 1970) are not considered to be consequential to this report as they underlie the salt deposits and do not contribute to surface effects.

The Detroit River Dolomite at the Point Hennepin brine field, is principally a sequence of dolomite, anhydrite, limestone and sandstone.

In southeastern Michigan, southwest of Detroit, the upper Detroit River is restricted to sequences of dolomite overlying limestone. The dolomite is generally porous and vuggy with zones of calcite crystals and black shale

laminations and fractures. For a detailed core description see Horvath (1957) and Bottoms (1959). The lower Detroit River is generally porous with vugs and gypsum fillings and numerous thin shale beds and fractured zones at the Point Hennepin brine field (Horvath, 1957; Bottoms, 1959).

The Sylvania Sandstone-Detroit River Dolomite contact ranges from gradational to sharp, the variations can be seen in outcrop and well core samples. The thickness and areal extent of the Sylvania Sandstone in Michigan is shown in figure 4. Areally, the Sylvania Sandstone can be considered to be a lenticular body having a northwest-southeast trend extending about 75 mi wide; it occupies southern Essex County in southwestern Ontario (Landes, 1951; Sanford and Brady, 1955). The Sylvania Sandstone is composed of medium- to coarse-rounded quartz grains cemented with varying proportions of carbonate. At the Point Hennepin brine field the top of the Sylvania Sandstone is dolomitic, mottled, light gray, weakly cemented and densely packed. Below, the unit is a very pure, white, friable to very friable (perhaps even loose sand pockets) with some well cemented zones. The lower Sylvania Sandstone is gradational into the upper Bois Blanc Formation. The Bois Blanc Formation at the Point Hennepin brine field consists of sandy dolomite at the top of the unit, color dark- to brownish-gray with white to grayish chert and fractured zones with some calcite filling of fractures are present near the top. Below, the Bois Blanc Formation sand is absent and the dolomite is found to be fine grained. The dolomite contains numerous fractures with gypsum and carbonaceous stylolites as well as black shale laminae and partings (Horvath, 1957).

The upper part of the Bass Islands Dolomite is thin bedded with local brecciation, gypsum and shale partings and laminae and occasional fractured zones.

The lower part of the Bass Islands Dolomite is fine grained, massive, argillaceous in places, with carbonaceous bands or partings widely distributed throughout and laminae of gray shale. The unit contains numerous fractures with traces of gypsum, fluorite and halite in the fractures. (See Kalafatis, 1958, for a detailed core description.)

The Salina Formation generally consists of gray to greenish-gray argillaceous dolomite, dolomitic shale, and brown to buff finely crystalline dolomite. Brown to grayish-brown limestone occurs near the base. Anhydrite is common throughout the formation. Red dolomitic shale and pink anhydrite, associated with greenish-gray dolomitic shale, form a consistent zone in the upper part of the formation. Beds of salt, representing the two main periods of salt deposition, are referred to as the "upper" and "lower" salt. Near the center of the Michigan Basin the thickness of the Salina Formation exceeds 4,500 ft with salt beds representing nearly half the total section. Near the Grosse Ile brine field the section is approximately 830 ft thick with salt representing nearly 30 percent of the section (Landes, 1951).

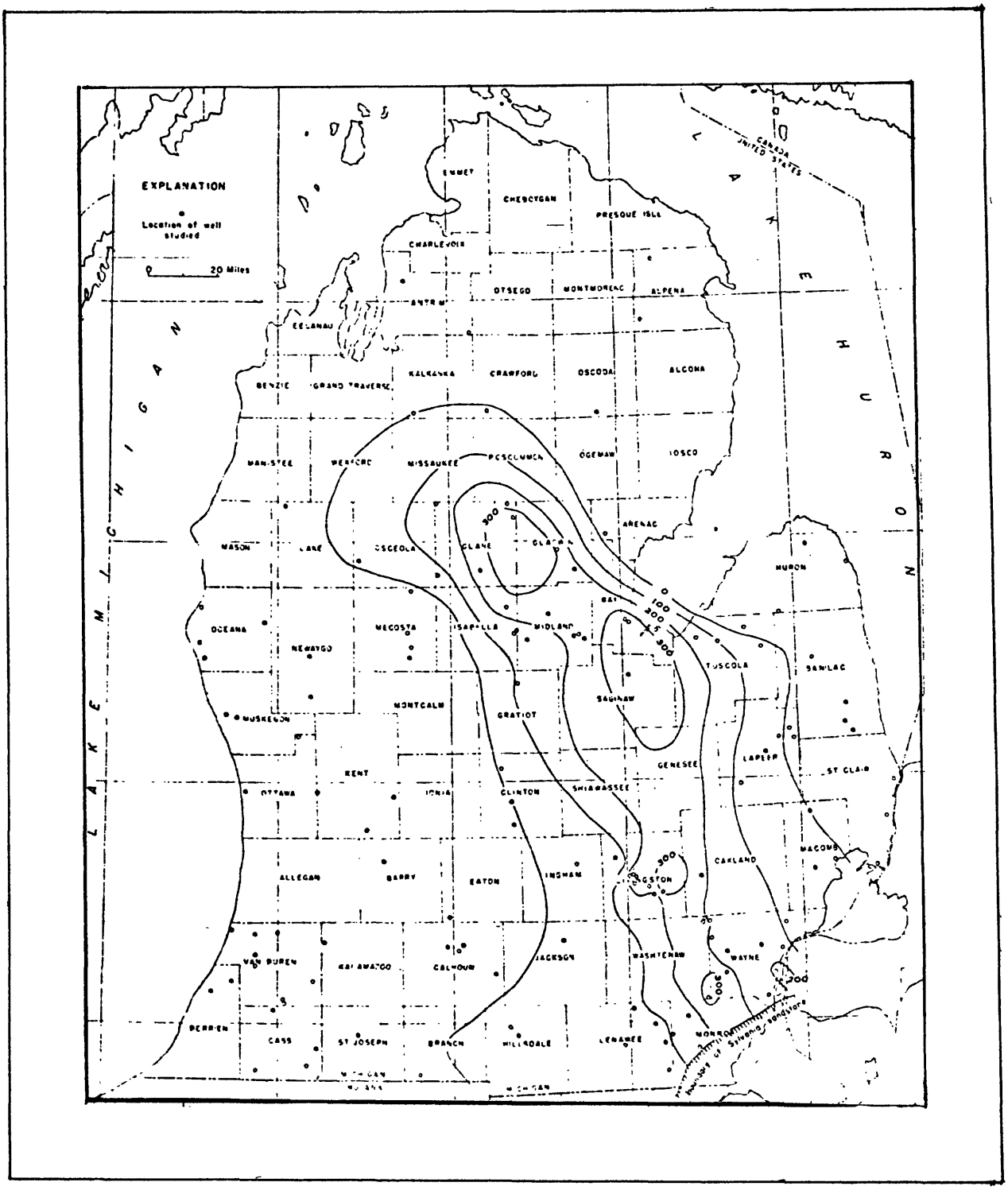

Figure 4.--Thickness of the Sylvania Sandstone (Landes, 1951). Contours in feet.

The Salina Formation has been subdivided from top to bottom into units G to A (Landes, 1945). The major salt beds are found in the F, D, and B units although all units contain salt to some degree. The vertical distribution of salt is shown in figure 1.

The Salina G unit is composed of compact, light-gray shaly dolomite with zones of denser dolomite of homogeneous texture with bituminous matter, gypsum, halite and pale-blue anhydrite throughout. Unit G is approximately 180 ft thick at the Point Hennepin brine field. Numerous fractures and fracture zones are observed throughout, with shale partings, gypsum vugs with occasional solution cavities, presumably resulting from ground water removal of disseminated soluble minerals.

The Salina F unit consists of salt beds separated by beds of brecciated dolomite, shaly dolomite and shale. The shales and shaly dolomites are generally thin beds of gray, green, or brown color. Anhydrite is present, especially conspicuous within the shales and shaly dolomites. The salt is nearly pure white. The dolomite beds are fractured with solution cavities present. Numerous shaly partings are found in the shaly dolomite beds.

The Salina E unit is composed of greenish-gray dolomite, mixed with anhydrite. Impure halite, brownish black, translucent with highly brecciated zones is present as well. Solution cavities are found throughout resulting in minor porosity. The dolomite and shaly dolomite are generally fractured and contain numerous shale partings.

The Salina D unit consists of nearly pure halite mixed in places with massive, finely crystalline dolomite. The dolomite contains numerous fractures and solution cavities with inclusions of halite, anhydrite and gypsum. The lower halite bed is mixed with soft, fine-grained dolomite.

The Salina C unit consists of massive greenish-olive-gray, shaly dolomite mixed with bluish sugary anhydrite. The shaly dolomite is fine to medium grained and mixed with reddish halite throughout and numerous fracture zones. Shale partings and massive anhydrite can be found in places.

The Salina B unit consists mostly of salt with alternating shaly dolomite beds. The shaly dolomite beds contain many solution cavities, and numerous fractures with occasional shale partings. The salt ranges from clear to black depending on the presence of minor impurities. The salt beds in the B unit are massive, transparent to translucent at the top to more impure at the base with alternating layers of greenish shaly dolomite.

The Salina A unit at Point Hennepin consists of massive, buff to grayish dolomite with some dolomitic limestone and sugary anhydrite. Some salt is found mixed with greenish-gray shaly dolomite. The dolomite has numerous carbonaceous inclusions with some fractures and bituminous partings present.

Units below the Salina Formation are not included in the lithologic description as these units are not disturbed by the solution mining activities confined to the Salina Formation evaporites and thus have no effect on the present topic discussion.

Structural Aspects

The State of Michigan is underlain by a nearly circular basin referred to as the Michigan Basin. Rock strata in the basin dip 0.5°-1.0° toward the center of the basin. The Point Hennepin brine field is located on the southeastern edge of the Michigan Basin. The rock strata gently dip to the northwest and minor warping of the strata is superimposed on the regional dip. There is no known major faulting within the proximity of the Point Hennepin brine field. The regional structure of the Michigan Basin has been discussed by Landes (1945), Newcombe (1933), Pirtle (1932), Smith (1937) and Lockett (1947). Due to low basinward dips beds are essentially horizontal. The major joints dip at a high angle and strike in a northeasterly direction.

Geologic History

The following review concerns only the history of the stratigraphic units of direct concern to this investigation, principally the depositional history of the Silurian Bass Islands Dolomite and Salina Formation and the Devonian Detroit River and Bois Blanc Dolomites.

At the beginning of Salina time (Late Silurian) the interior sea formerly covering what is now the midcontinental United States was retreating and sufficient land had emerged so that numbers of landlocked salt-water lakes remained, surrounded and separated by broad expanses of arid land. The Michigan Basin was covered by one such lake. By one theory, evaporation greatly exceeded inflow from streams resulting in concentration of minerals in the water, which in turn, led to the deposition of dolomite, calcium sulfate and salt. The extensive deposits of salt and anhydrite found in parts of the Salina Formation are thought to be the result of periodic or continuous influx of sea water with subsequent evaporative concentration or perhaps the sediments and concentrates that constitute the Salina deposits were deposited in playa-type lakes surrounded by widespread desert land subject to long-continuous erosion and drainage by intermittent streams that flowed into lakes. Thus the pre-Salina marine sediments may have been dissolved and transported to the lakes to be concentrated and deposited by evaporation as they are deposited in similar basins today.

It should be noted that this discussion does not provide for massive thicknesses of pure salt found in the Michigan Basin, nor does it explain absence of typical dessication minerals, complex salts, potash, or magnesium minerals.

A disconformity exists between the Salina Formation and the Bass Islands Dolomite but the beginning of Bass Islands time was expressed by little change in climate or physiography. The sea again covered southern Michigan and fossil evidence indicates westward transgression. With an increasingly moist climate, drainage exceeded evaporation and dolomitic slime and clay muds were washed into the basin. Layers and films of carbonaceous matter interstratified with the dolomite indicate the presence of vegetation. Ripple marks and desiccation cracks on the surface of some strata indicate a shallow water and even mud-flats environment.

The shallow water condition of the late Bass Islands-Bois Blanc time culminated in a second emergence of southern Michigan with establishment of desert or semidesert conditions. One to two transgressions of the sea occurred and the erosion effects on such strata as the previously existing Ordovician St. Peter Sandstone and the Precambrian Baraboo Quartzite allowed removal of the pure quartz material to the Michigan Basin area to form the Sylvania Sandstone. This rather large area of sand was deposited into dunes which were crossbedded and irregularly stratified. With eventual subsidence and transgression of the sea, the sands were to a degree reworked. Subsequent percolating water introduced silica, calcium and magnesium carbonates but the low permeability accounts for the varying degree of cementing observed today in the Point Hennepin area.

The dolomitic beds of the Detroit River Dolomite were laid down upon the Sylvania Sandstone with introduction once again of a more humid Bass Islands-like time. The dolomites and limestones exhibit varied origins from that of limestone beds so pure, compact and delicately laminated as to suggest a chemical precipitate to other beds rich in animal remains (Dorr and Eschman, 1970).

SYLVANIA SANDSTONE

The Sylvania Sandstone is typically a remarkably pure, sparkling, snow white aggregation of coherent to loosely coherent quartz sand. Lumps of the sandstone can be easily crumbled. An eolian mode of deposition of the Sylvania Sandstone is the most widely accepted. Much evidence supports this mode of deposition. There is an increase in thickness of the Sylvania from southeast Michigan and northwest Ohio towards the northwest and a decrease in thickness in all other directions. The erosion of some previously formed pure sandstone or quartzite such as the Ordovician St. Peter Sandstone or Precambrian Baraboo Quartzite by wave action and the transport of the grains of quartz by prevailing northwesterly winds could give rise to the Sylvania. During retreat of the shoreline, winds would carry the grains to sea where they would have intermingled with the accumulating dolomitic slime, subsequently forming the siliceous dolomite which underlie or form the base of the Sylvania Sandstone. A pronounced retreat allowed deposition of the Sylvania Sandstone. The eventual return of the sea closed the Sylvania episode and the upper layers were reworked by waves and horizontally

stratified with finer sediments and fossils being introduced locally. Crossbedding of windblown deposits is not uniformly inclined in one direction or in a uniformly varying direction. The Sylvania Sandstone exhibits random variation in the direction of inclination, including repeated reversals. The only subaqueous deposit with structure comparable to that of a windblown deposit is a wave-built bar. The Sylvania Sandstone is distributed over too large an area to have a bar origin. The great irregularities in the thickness of the beds, as between neighboring wells, is expected with eolian deposition but not so for a subaqueous deposition mode. The uniformity in the grain size (fig. 5) of the Sylvania Sandstone is difficult to attribute to any theory of water deposition. The absence of clay, the complete rounding of the smaller grains and the pitted character of the coarser grains, when not hidden by secondary enlargement, point to continued wind action. Plots of grain-size distribution of the Sylvania Sandstone in the southeast Michigan area shows a progressive decrease in grain size to the southeast as would be expected by the eolian mode of deposition. Comparison of the Sylvania Sandstone grains with the St. Peter grains from Missouri, Illinois, Wisconsin, and Minnesota reveal that the St. Peter Sandstone grains are not as completely rounded and sorted (Grabau and Sherzer, 1910, pl. 7). The absence of shale deposits about the margin of the Sylvania Sandstone, an abnormal eolian feature, can be explained by the purity of the source material (St. Peter) with a percentage silica of sometimes 99 percent.

The small amount of cement consists of dolomitic material or calcite, deposited secondarily by percolating water. Descriptions of the body of the Sylvania Sandstone by various investigators (for example, Grabau and Sherzer, 1910; Reavely and Winder, 1961; Carman, 1936) revealed the Sylvania Sandstone cohesion as being highly variable from one location to another. At Point Hennepin, the material varies from coherent to loosely coherent. An analysis of the sandstone from Monroe County, Mich. is shown in table 1.

Table 1.--Analysis of Sylvania Sandstone

[After Sherzer and Grabau, 1909]

	Percent
Silica	96.50
Calcium carbonate	1.50
Magnesium carbonate	1.04
Iron oxide	.00
Sulfuric acid loss and undetermined	.76
Loss on ignition	.20
	100.00

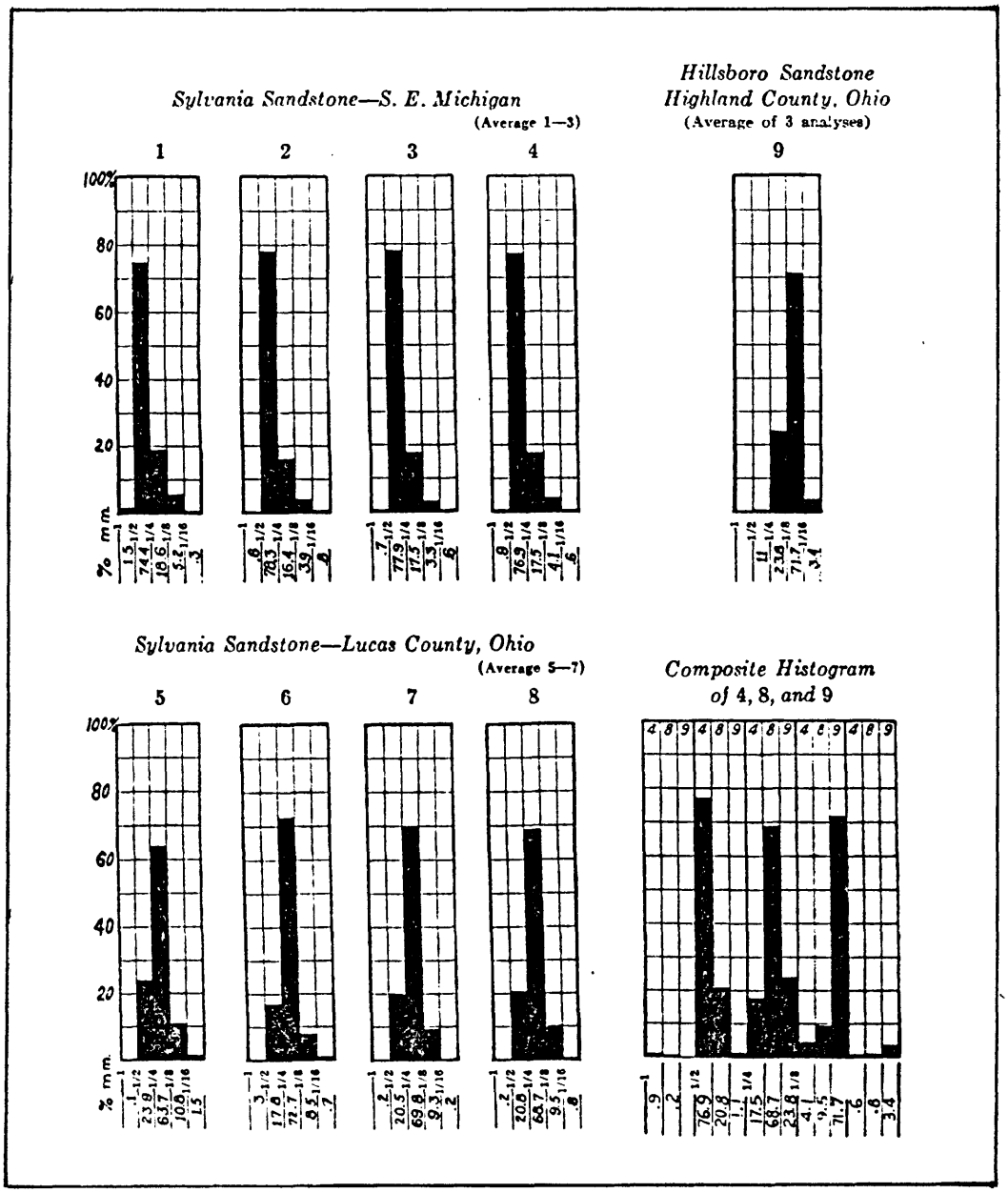

Figure 5.--Size of grain and degree of sorting for various samples of Sylvania and Hillsboro Sandstones, shown by percentage distribution. Numbers 1, 2, and 3 show analyses of samples of Sylvania Sandstone from southeastern Michigan; number 4 is the average of these three. Numbers 5, 6, and 7 represent samples of Sylvania from northwestern Ohio; number 8 is the average of these three. Number 9 records the average of three analyses of the Silurian Hillsboro Sandstone from southern Ohio. The composite histogram of 4, 8, and 9 shows the relative size, and the percentage falling into each of the several grade sizes, for the Sylvania Sandstone of southeastern Michigan, the Sylvania of northwestern Ohio, and the Hillsboro of southern Ohio (after Carman, 1936).

SCOPE OF LABORATORY TESTING

Since the main effort of the present study was to critically examine the role of the Sylvania Sandstone in surface sink development, extensive laboratory testing was planned to determine various physical properties and to determine features such as degree and type of cementing with depth, type of grain boundaries, etc.

NX-size core samples of Sylvania Sandstone taken from experimental core hole No. 2 were made available for testing. Direct observation of the core, stored at a warehouse on Point Hennepin, revealed that the physical properties of the Sylvania Sandstone varied considerably through its thickness. The top and bottom of the Sylvania Sandstone had far greater resistance to crumbling with finger pressure than the material in the middle. The zone of the Sylvania Sandstone, at one-fourth to one-third of the thickness from the top of the unit consisted of a mixture of loose sand and small 0.5-1 in. irregularly shaped broken pieces, indicating that, although friable, the material had some cohesion and that the coring operation introduced stresses sufficient to cause material failure.

The obvious physical property variation prompted the development of an extensive testing program to determine the variations of strength properties of the Sylvania Sandstone with depth.

The laboratory analyses consisted of uniaxial testing, triaxial testing, direct shear testing, indirect tensile testing, thin section analysis, and sand-water slurry testing. The NX core was taken to the structural testing facilities at the Geology Department at the University of Illinois, Urbana, Ill.

Uniaxial Testing

Uniaxial testing resulted in a range of unconfined compressive strengths of dry Sylvania Sandstone as shown in figure 6. The Sylvania Sandstone exhibits fairly high (6,000-8,000 lbf/in^2) unconfined compressive strengths at the top and bottom with values dropping to unknown low values in the zone from which no adequate test specimens were available.

As noted in figure 6, the lowest value of unconfined compressive strength measured was approximately 1,200 lbf/in^2 An average value of unconfined compressive strength based on measured data is approximately 3,000 lb/in^2

Of particular note was the manner in which samples failed during the uniaxial testing. In all cases of compressive type failure the specimens failed explosively and, more significantly, in excess of 50 percent of the samples became loose granular sand (fig. 7).

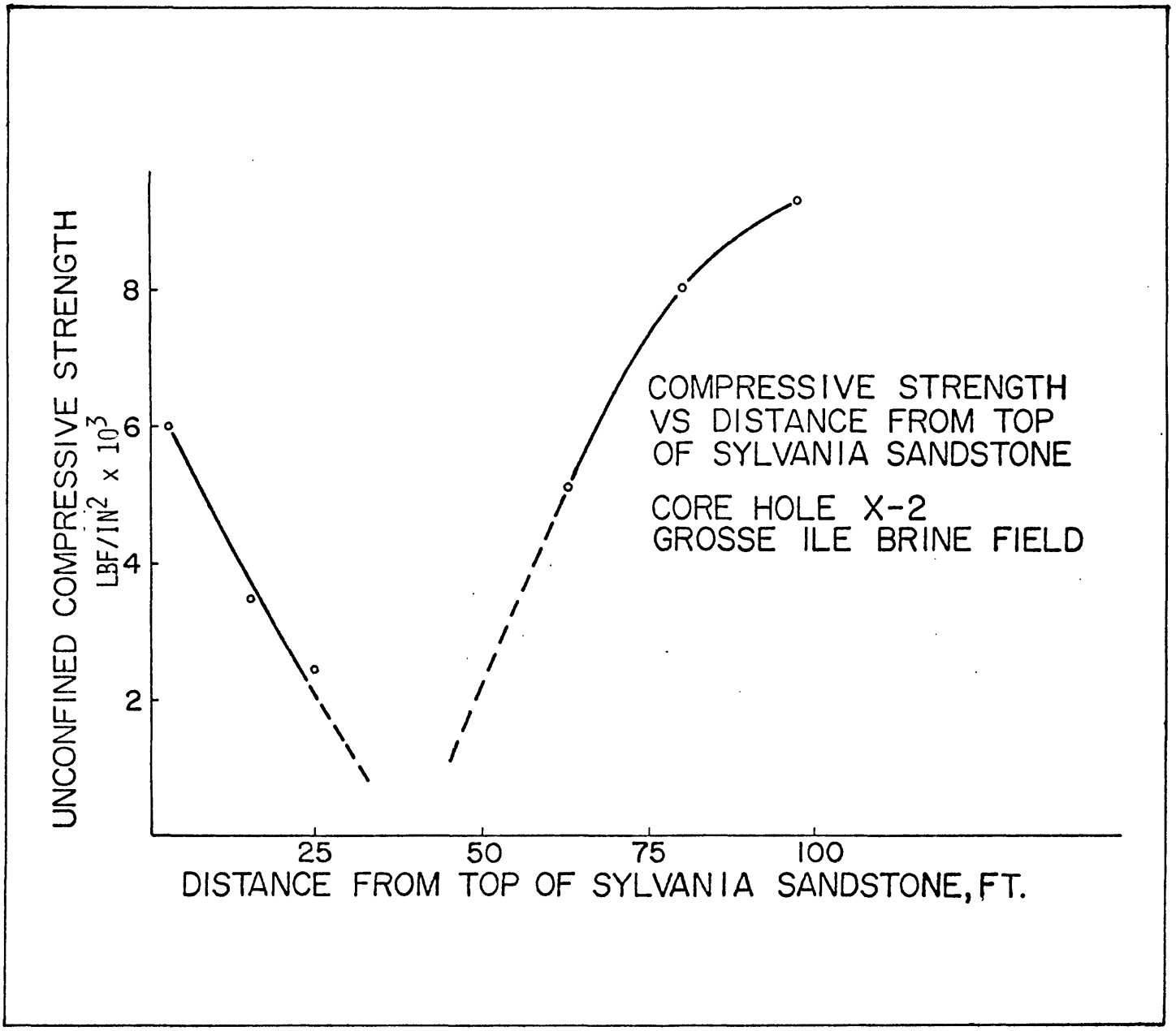

Figure 6.--Unconfined compressive strength of dry Sylvania Sandstone versus depth within Sylvania Sandstone unit.

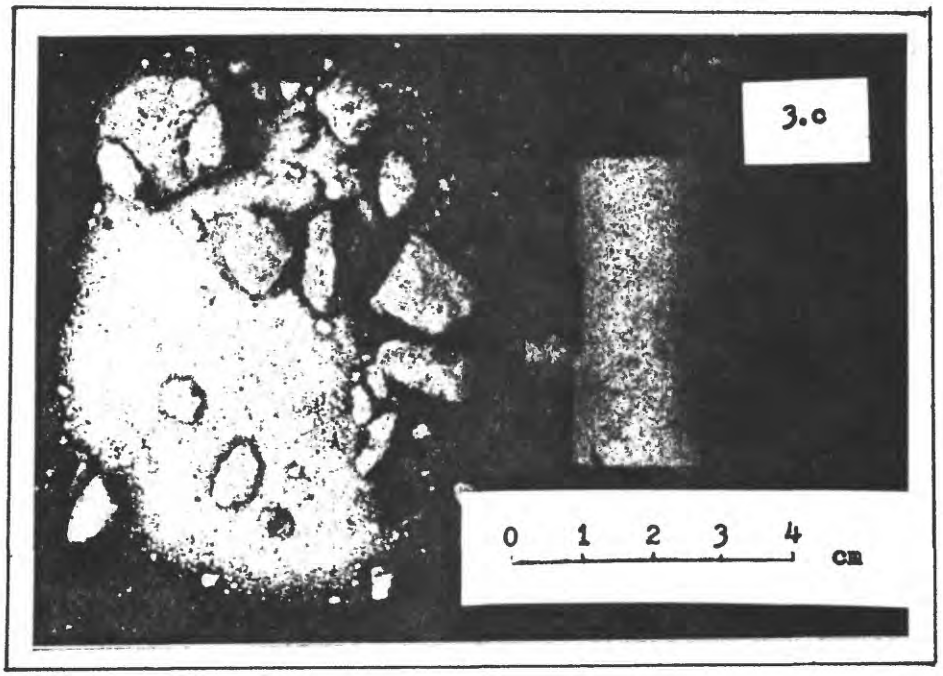

Figure 7.--Photograph showing Sylvania Sandstone core sample before and after uniaxial testing to failure.

Sample preparation consisted of diamond-drill coring with water circulation and slab sawing with water circulation with subsequent oven drying for 24 hours at 70°C. Testing of the samples was in the dry condition.

Samples for uniaxial and triaxial testing consisted of cylindrical specimens of 1 in. diameter and 2 in. long, representing the entire thickness of Sylvania Sandstone. It should be noted, however, it was not possible to test specimens within a 20-ft zone, approximately 0.25-0.33 the distance from the top of the Sylvania Sandstone unit, as the fragments, as previously mentioned, were too small for sample preparation.

Triaxial Testing

Triaxial tests were run at confining pressures that simulated the overburden encountered in situ at the Point Hennepin brine field. The range of confining pressures was 100-200 lbf/in^2. The failure mode was again of the same nature as that of the uniaxial test specimen.

Two samples of Sylvania Sandstone NX-size core, approximately 4 in. long, were instrumented with paperbacked electrical strain gauges in the axial and circumferential direction to determine Poisson's ratio. These samples were tested under compression with load and strains recorded simultaneously at 500 lb force increments (fig. 8). Poisson's ratio values in excess of 0.5 were measured even at very low normal loads and as high as 1.0 at higher loads indicating a highly dilatant material. The dilatant behavior of the Sylvania Sandstone has been corroborated by independent laboratory tests conducted by the U.S. Geological Survey.

Direct Shear Testing

Rectangular samples approximately 5 in. long by 0.5 in. thick by 1 in. high were tested in the direct shear apparatus shown in figure 9a (Nieto-Pescetto, 1974). With normal loads expected at in situ overburden depth, echelon-type tensile failures resulted (fig. 9b).

Indirect Tensile Testing

The core sample was slabbed into 1-in. discs and these discs were used as test specimens for Brazilian indirect tensile tests. Tensile failures (fig. 10) were clean with no tendency to form loose sand.

Thin Section Analysis

Thin sections taken from samples throughout the Sylvania Sandstone unit revealed an extraordinary degree of pressure solution (fig. 11). Thin sections were oriented in both the vertical and horizontal planes and examination revealed no preferential direction of pressure solution. The grains are uniformly pressure welded throughout the unit. Figures 12a and 12b show the uniformity of grain boundary pressure solution with depth.

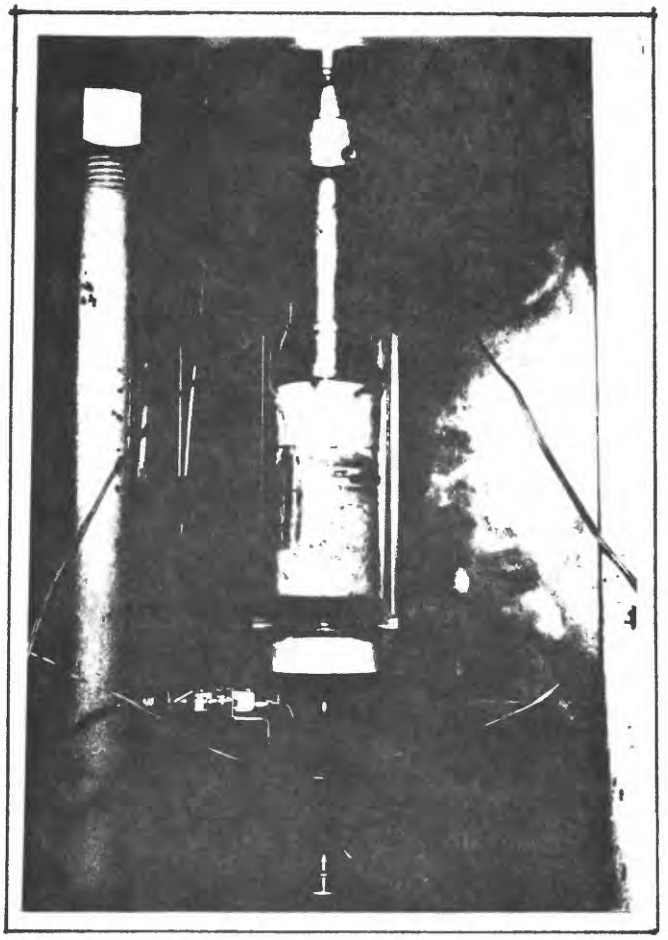

(A)

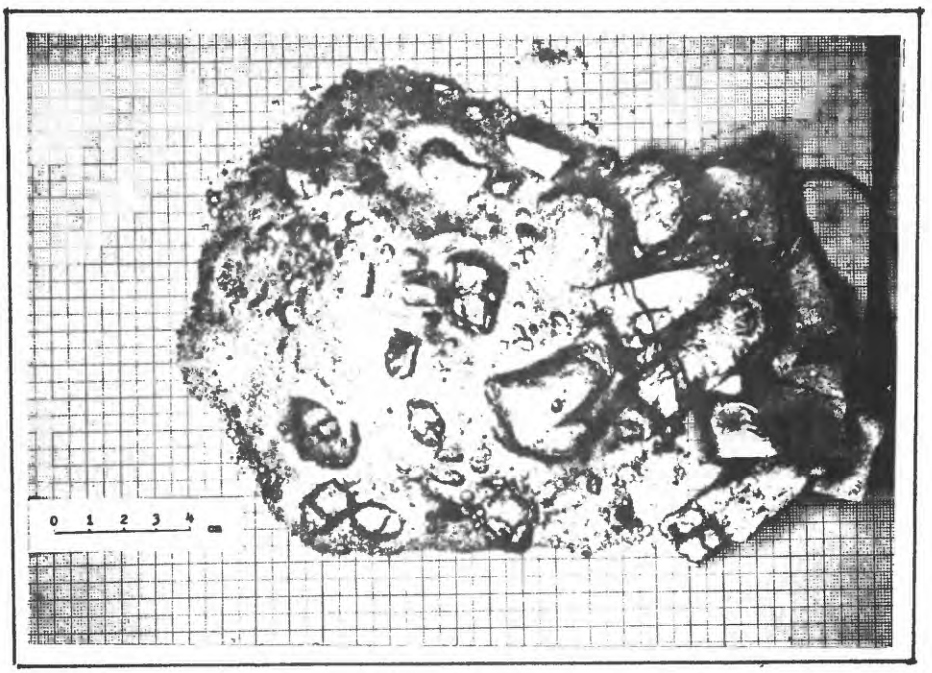

(B)

Figure 8.--Photographs of a) NX-size core sample of Sylvania Sandstone instrumented with paperbacked electrical strain gauges prior to uniaxial testing and b) same NX-size core sample after test to failure.

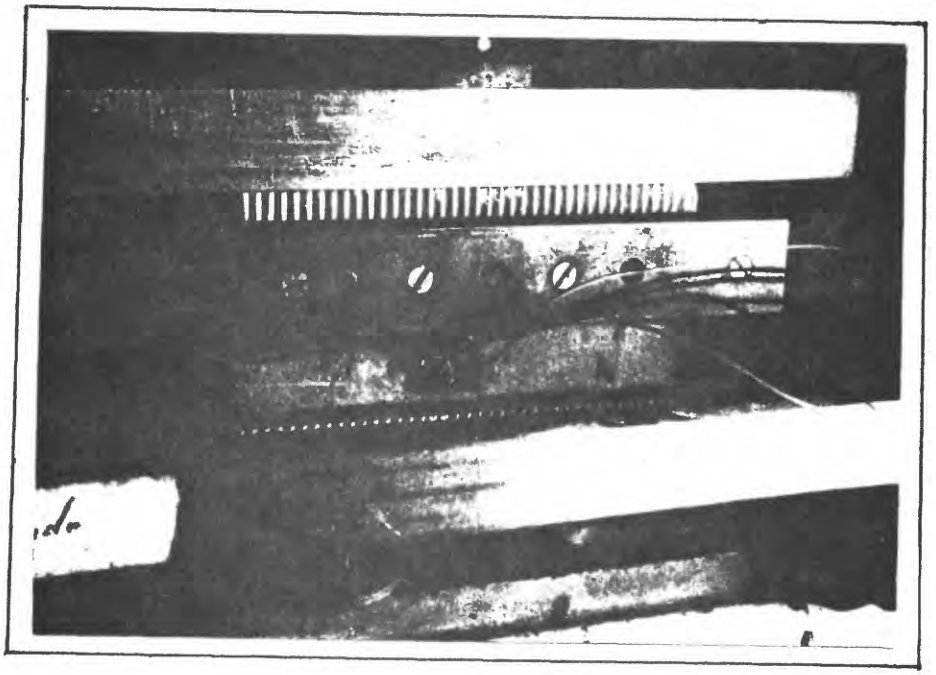

(A)

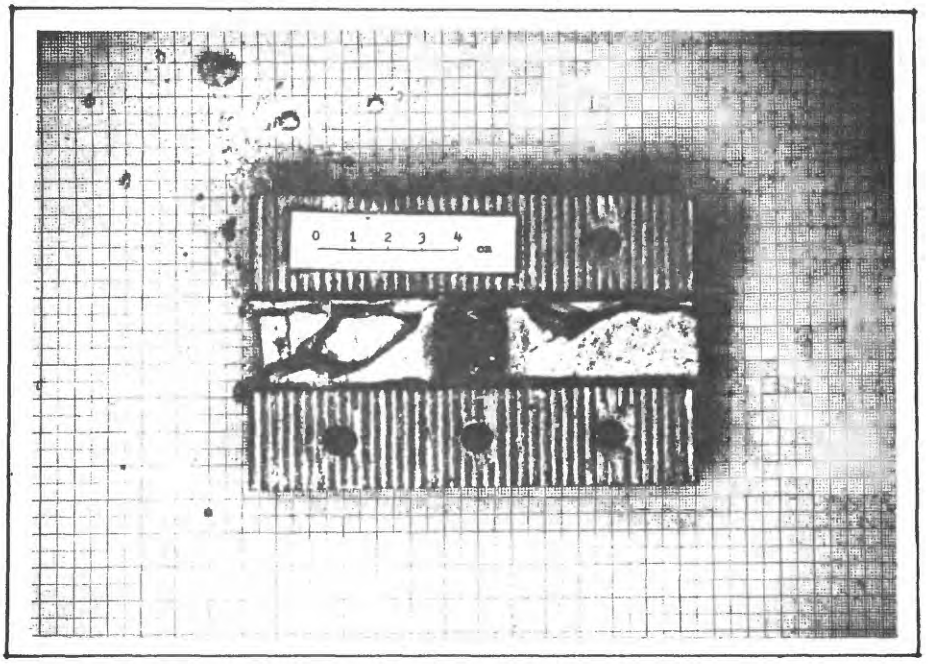

(B)

Figure 9..--Photographs of a) rectangular sample of Sylvania Sandstone prior to direct shear testing and b) same sample after test showing echelon tensile failures.

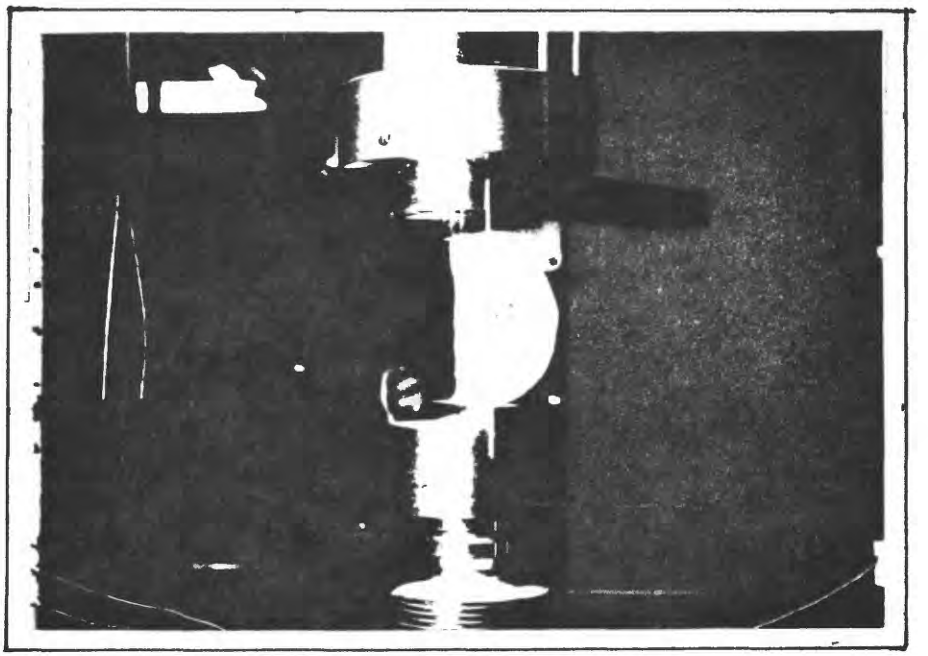

Figure 10.--Photograph of indirect tensile test (Brazilian) showing clean break with no loose sand generated.

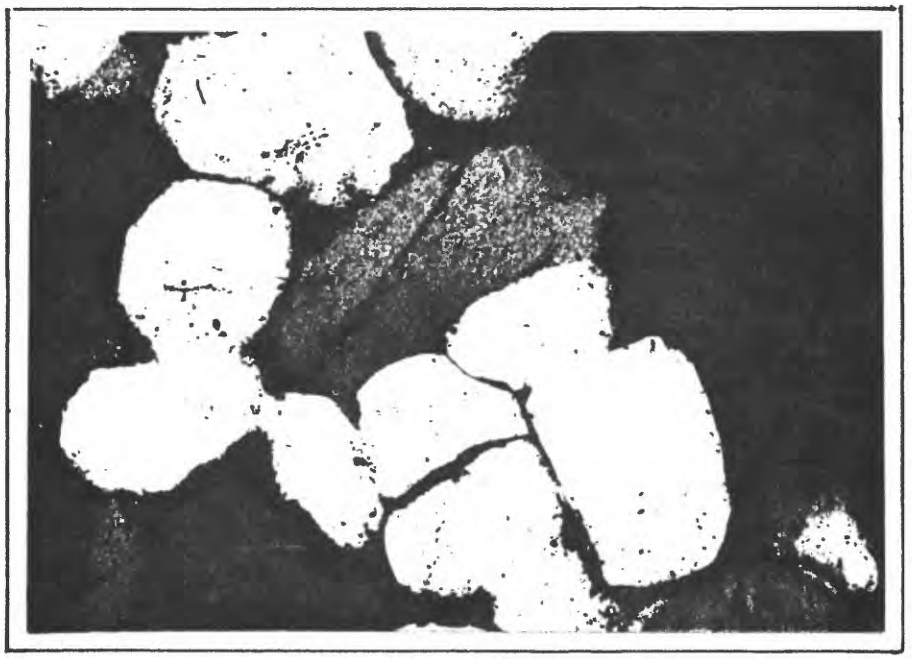

Figure 11.--Photomicrograph (X40) of quartz grain boundaries showing pressure solutioning.

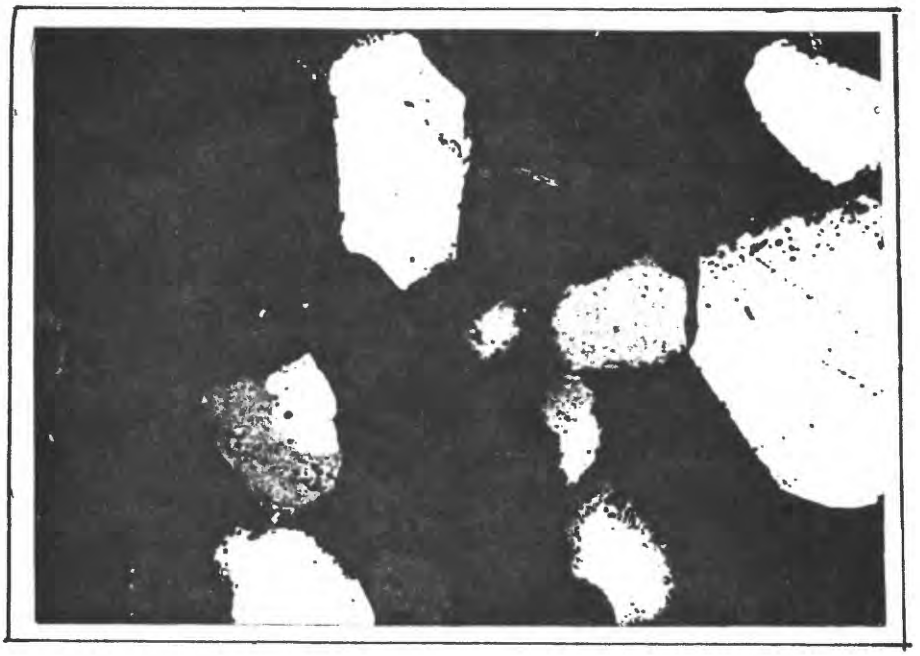

(A)

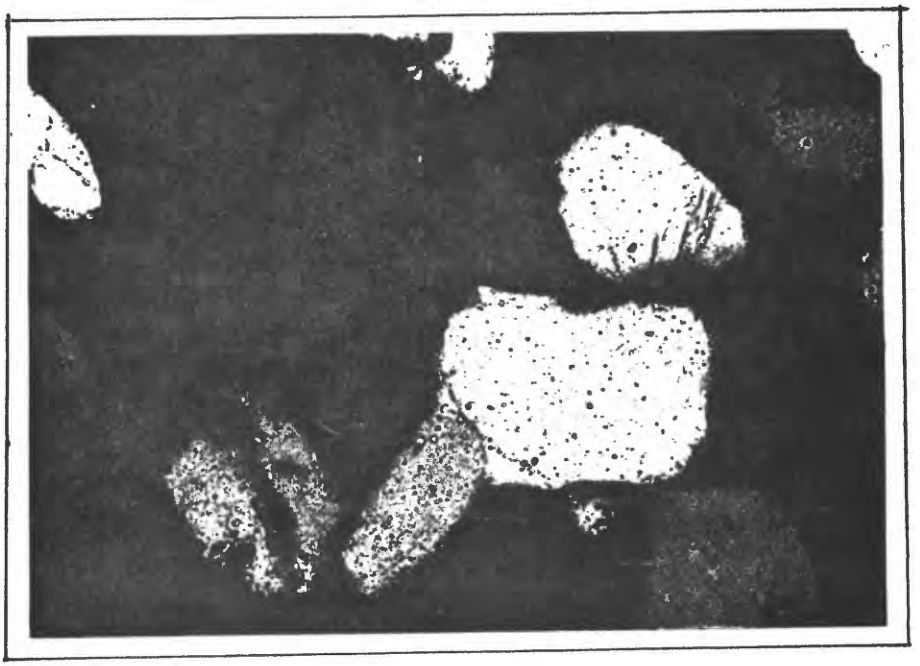

(B)

Figure 12.--Photomicrographs (40X) of a) quartz grains in planar contact due to pressure solution at a depth of 50 ft from top of Sylvania Sandstone unit, b) quartz grains in planar contact due to pressure solution at a depth of 85 ft from top of Sylvania Sandstone unit.

Figure 13 shows a X40 magnification of the grain boundaries illustrating the high degree of silica overgrowth and the remarkable absence of any calcite cement. Secondary calcite cement, when present, is very sparse as would be expected due to the high degree of pressure solution (fig. 14) causing low permeability and inhibiting ground-water flow.

Microscopic examination of grain boundaries yielded no hint of the unusual variation in unconfined compressive strength throughout the Sylvania Sandstone. The variation must be reflected in the suture zone of grain to grain boundaries which would be observable in X-ray microscopy. This effort was not undertaken.

Variations of porosity and void ratio with depth within the Sylvania Sandstone were determined statistically from the thin section point counts. The average porosity was 10 percent. Porosity and void ratio with depth within the Sylvania Sandstone is shown in table 2.

Table 2.--Measured values of porosity and void ratio versus depth at Sylvania Sandstone

Depth (ft)	Porosity (n)	Void ratio (e_o)
10	9.4	0.104
20	11.4	.129
43	7.92	.086
65	9.77	.108
72	11.1	.124
84	9.4	.104
100	8.89	.097

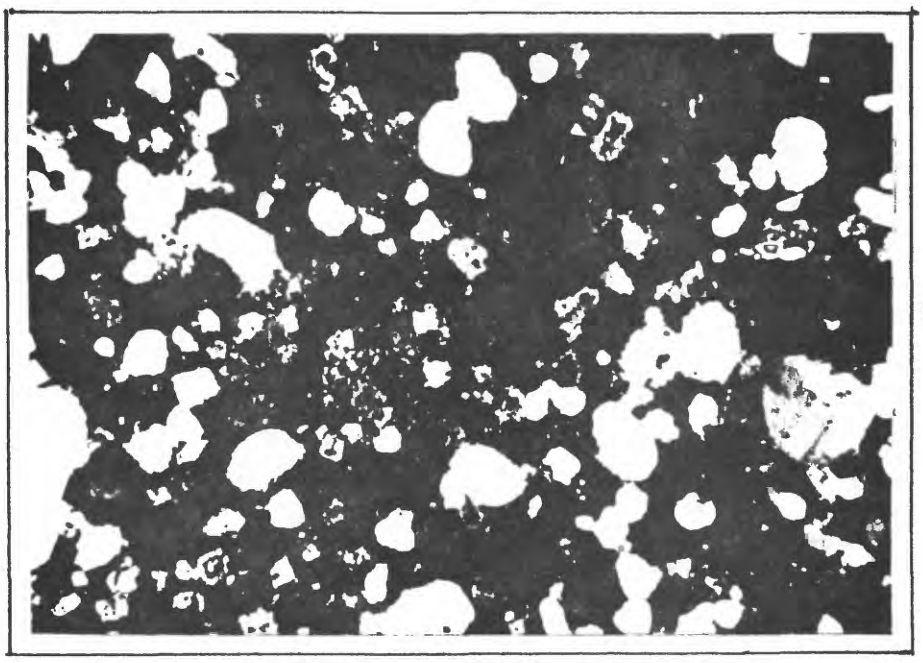

(A)

(B)

Figure 13.--Photomicrographs showing a) zone of silica overgrowth, 10X and b) greater detail (40X) of silica overgrowth of zone identified in (a).

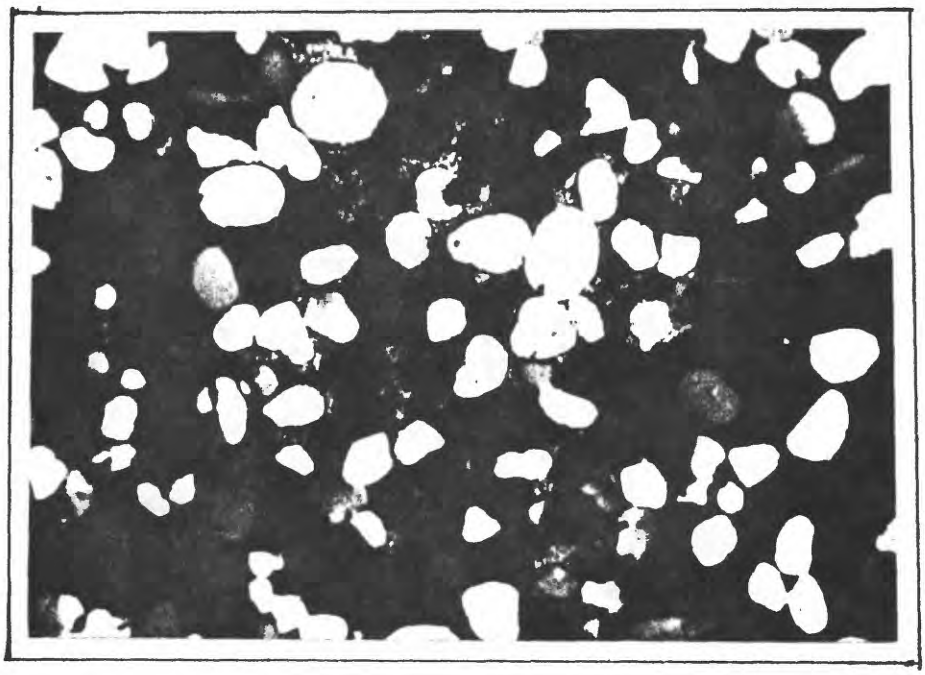

Figure 14.--Photomicrograph showing the sparse presence of secondary calcite in quartz grain matrix.

Discussion of Mechanical Properties and In Situ Stress

The unique configuration of the sandstone grains is believed to account for the unusual mechanical properties of the Sylvania Sandstone reported in the section above. As the sandstone is loaded in compression, either by direct loading in a uniaxial or triaxial apparatus or indirectly as a result of general subsidence over a broad area, the dilatant behavior of the sandstone indicates that the grains rotate relative to one another with loading. As the load increases, a point is reached when failure commences and the stored elastic strain energy is released with the dramatic consequence of greater than 50 percent of the matrix being reduced to loose granular sand.

Laboratory testing of all samples followed oven drying of the samples for 24 hours at 70°C. However, in situ, the Sylvania Sandstone is within the water table and thus saturated. Therefore, reductions of compressive strength values obtained by testing to account for loss in strength because of wetting is warranted. Table 3 (Boretti-Onyszkiewicz, 1966) shows that for saturated sandstones an average reduction of compressive strengths of 35 percent can be expected. Further, there is an additional reduction in strength because loading in the laboratory tests was directed perpendicular to bedding, whereas loading in situ is parallel to bedding.

Figure 15 shows the maximum compressive strength versus depth for a saturated Sylvania Sandstone tested parallel to bedding based on the hypothetical 40-50 percent reduction of compressive strength previously mentioned.

In situ stress measurements that have been made in the vicinity of the Michigan Basin indicate the existence of high horizontal stresses (Franklin and Hungr, 1978). In a summary of rock stress data in Canada, Franklin and Hungr (1978) refer to in situ stress measurements taken in Paleozoic carbonate and shale rocks in nearby Ontario and list variations in horizontal stresses with overburden depths (p. 28). High horizontal stresses in the range of 1.7-14.7 MPa have been measured at shallow depths between 2-37 m within 350 km of the Windsor-Detroit area. Generally only a small difference in magnitude between the two horizontal principal stress components has been found. The major principal stress direction seems to be fairly constant throughout the region, with a northeast to easterly trend. Herget (1973) and Herget, Pahl and Oliver (1975) have proposed the following empirical equation for relating average horizontal stress to depth below ground surface based on Canadian values

$$\sigma_H = 8.16 \text{ MPa} + 0.04 \text{ H MPa}$$

where H = depth in meters.

State	Sample 1		Sample 2		Sample 3		Sample 4		Sample 5	
	Perpendicular to stratification	Parallel to stratification	Perpendicular to stratification	Parallel to stratification	Perpendicular to stratification	Parallel to stratification	Perpendicular to stratification	Parallel to stratification	Perpendicular to stratification	Parallel to stratification
In air-dry state.	150.2 (21783)	137.3 (19908)	125.6 (18219)	88.4 (12823)	93.9 (13618)	99.4 (12965)	93.5 (13561)	83.2 (12070)	69.2 (10039)	54.5 (7909)
After water saturation.	103.7 (15038)	92.5 (13419)	87.9 (12752)	76.5 (11090)	63.4 (9202)	53.5 (7753)	81.4 (11800)	65.1 (9443)	55.2 (8009)	50.3 (7299)

(Compressive strength of samples in MPa (lbf/in^2)).

Table 3 Compressive strength of a sampling of sandstone showing wet vs. dry strength, loaded both perpendicular and parallel to the bedding. (Modified from Boretti-Onyszkiewicz, 1966).

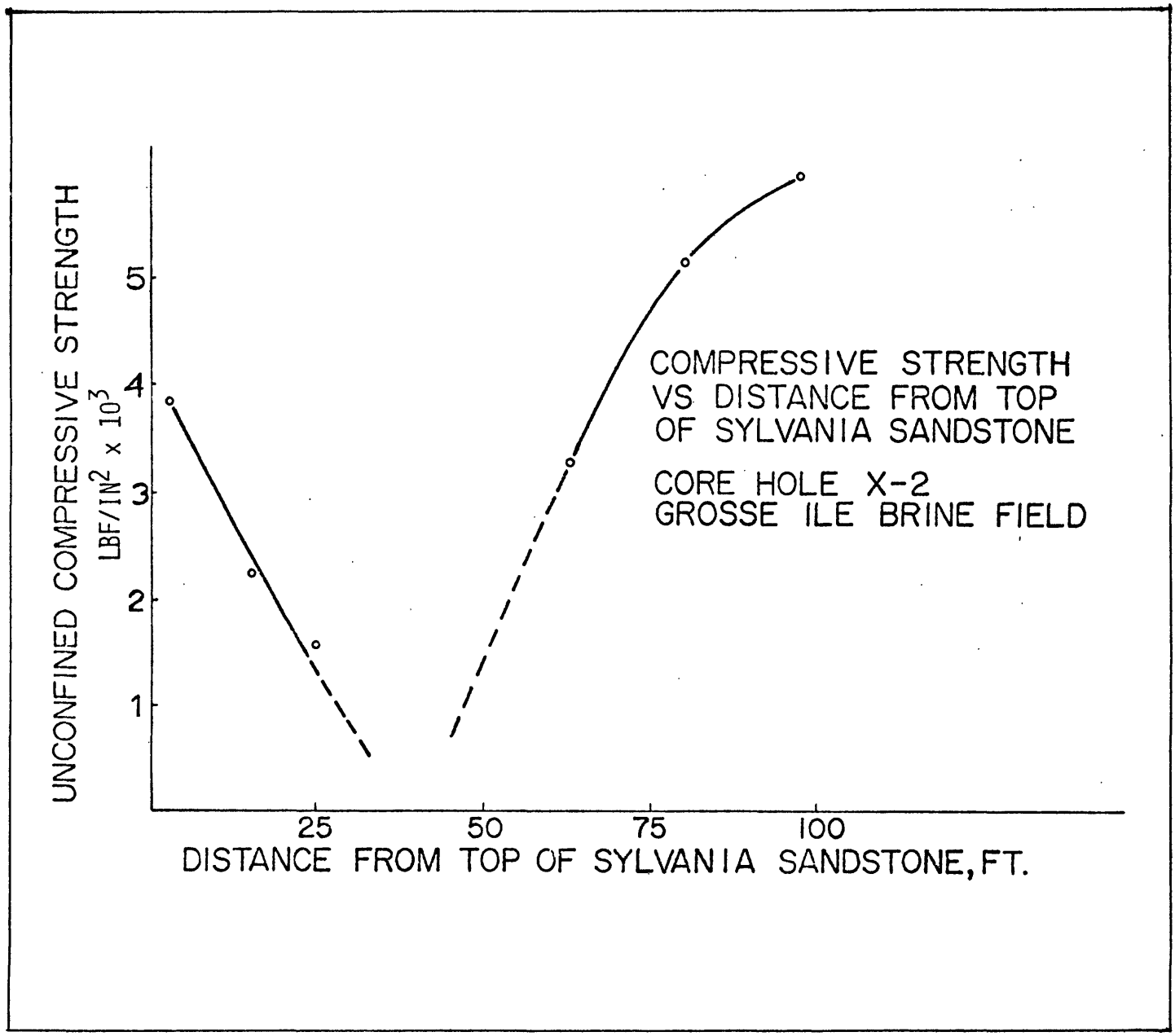

Figure 15.--Unconfined compressive strength of saturated Sylvania Sandstone tested parallel to bedding versus depth within Sylvania Sandstone unit.

The zone of low-compressive strength Sylvania Sandstone is at an average depth of 275 ft below ground surface at Grosse Ile. Using values obtained from the above equation, the Sylvania Sandstone at this depth could be horizontally loaded to at least 1,500 psi in the natural state, that is prior to any horizontal loading caused by solution-mining induced deformation. At that depth the Sylvania Sandstone has unaxial compressive strengths ranging from approximately 1,400 to 5,000 psi. Thus the weak zone of the Sylvania Sandstone is initialy under a horizontal compressive stress of nearly the ultimate unconfined compressive strength. The material, however, has some confinement caused by the overburden. Any deformation that would increase horizontal stresses and (or) decrease the confining effect of the overburden could bring the sandstone very close to failure.

Sand-Water Slurry Tests

Although the Sylvania Sandstone, the Detroit River Dolomite and the Bois Blanc Formation are known to contain many high-angle joints and fractures, the question persisted as to how large quantities of Sylvania Sandstone were removed in the form of loose granular sand due to compressive failure. Transport of the loose sand was paramount to the hypothesis of creating an expansive shallow-depth cavity that could in turn lead to surface sink formation.

Simple gravity flow tests of water-sand were conducted to obtain a qualitative understanding of the migration of loose granular sand down the near vertical joints and fractures known to exist in the Sylvania (fig. 16) and also known to continue in the underlying dolomite. In a plexiglas tank of approximately 8 in. wide, 36 in. long, and 18 in. deep, artificial rock (Sulfaset) blocks were arranged to specific gap widths through which sand-water slurry could migrate vertically downward.

Due to the lack of quantities of loose granular Sylvania Sandstone sand and the availability of St. Peter Sandstone sand it was decided to complete testing by using the St. Peter sand and extrapolating the data to the Sylvania sand as a model of the sand migration process. The individual tests consisted of using shim stock between Sulfaset blocks to maintain gap geometry and placing a thin plastic sheet that could be easily slid away from under the sand. The blocks and gap were damned with 1-in. barriers around the periphery allowing approximately 16 $in.^3$ of sand to be stored above the blocks and gap. The tank containing the blocks was filled with water. The blocks were elevated above the tank bottom to allow continual flow of sand. Removal of the plastic sheet allowed sand to move vertically downward. With a gap of 0.080 in., the sand continued to move down the gap through the still water with the process ceasing when the angle of repose of the slope of sand adjacent to the gap was approximately 35°. The St. Peter sand used in the

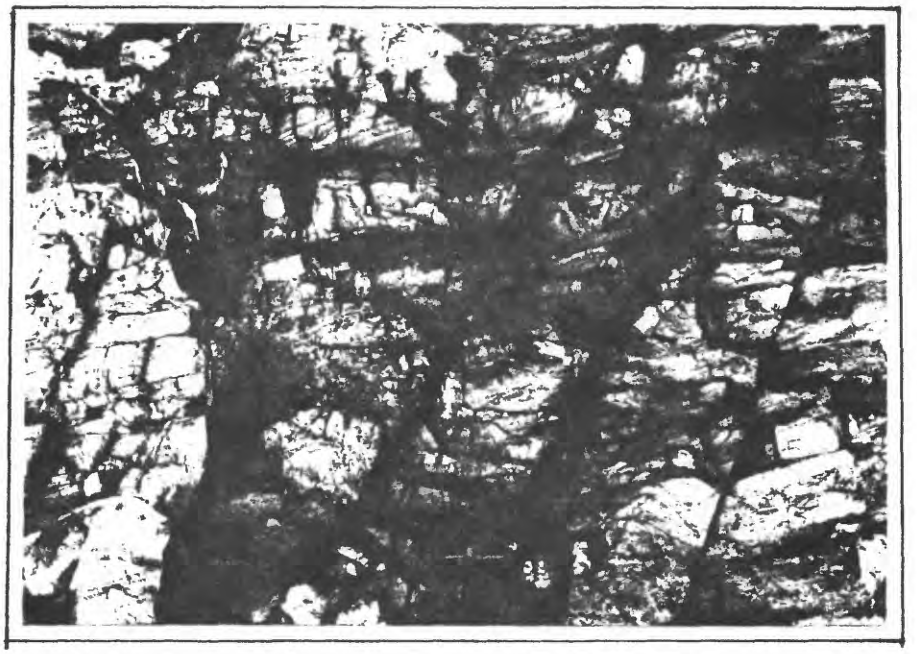

Figure 16.--Photograph of face of Sylvania Sandstone located in Rockwood Quarry showing high-angle northeast-trending joint sets.

testing consisted of well-sorted sand with a maximum diameter of 1 mm (0.040 in.) whereas the Sylvania sand maximum diameter found at Point Hennepin is 0.5 mm (0.0197 in.). Testing an array of gap widths demonstrated that a gap widths of 2 mm (0.080 in.) gap represented a gap of two times (2X) the maximum St. Peter sand grain size.

MECHANICAL MODEL FOR SINK DEVELOPMENT

In choosing a mechanical model of the behavior of the Sylvania Sandstone that may or may not result in surface sink development one must evaluate the evidence available. Efforts at mechanically modeling the Sylvania were made to account for laboratory measurements and other data.

Detailed descriptions (Horvath, 1957) from a core drilled at the Point Hennepin brine field indicates a zone of horizontal shale beds 0.5-0.25 in. thick approximately 9 ft above the base of the Sylvania Sandstone. These shale beds lie within a sandstone lens in the stronger sandy dolomite at the base of the Sylvania Sandstone. The presence of these low shear strength shale beds could allow lateral movement of the Sylvania Sandstone with respect to the lower part of the Bois Blanc Dolomite under the influence of the shear stresses induced by the general subsidence movements. These thin shale beds would be considered the base of a structural unit for any mechanical modeling of the Sylvania Sandstone.

The laboratory evidence (figs. 6, 15) of a relatively low compressive strength zone in the Sylvania Sandstone approximately 25 ft below the top of the Sylvania Sandstone unit leads to choosing this zone of weaker material as the top of a plate or beam model. This choice is corroborated by the field evidence (D. J. Dowhan, written commun.,, 1976) of a cavity observed in experimental borehole X-5.

As a first approximation to modeling the behavior of the Sylvania Sandstone under the stress fields imposed by general subsidence, beam and plate theory were considered.

Cavity size increase due to coalesence of individual cavities is a gradual process. Likewise, the gradual sagging of the brine cavity roof rock occurs in a gradual manner as the size of the brine cavity increases in areal extent.

The Sylvania Sandstone, which for the purposes of the analysis can be considered in cross as a beam or plate, first responded elastically to the downwarp of the underlying dolomite. Therefore, elastic theory was felt appropriate to determine stress fields. Since the modulus of the sandstone is less than the modulus of the underlying dolomite, the sandstone would initially follow the downwarp of the lower dolomite. The shale zone at the base of the Sylvania Sandstone would allow lateral movements and could thus be considered the base of the plate or beam. The low compressive strength zone, as previously discussed, would become the top of the plate.

As the Sylvania Sandstone begins responding elastically to the downwarp, a point is probably reached where the low strength zone can no longer maintain its integrity. This process is visualized to occur as follows: a horizontal separation occurs whereby the topmost 25 ft of Sylvania Sandstone will remain adhered to the Detroit River Dolomite and react with this higher modulus material while the lower Sylvania Sandstone continues to respond to the downwarp of the dolomite below. In the low strength zone the vertical stress is reduced from the overburden stress to effectively zero stress when the opening is formed. Since the top of the plate or beam is no longer confined, unconfined compressive strengths of the Sylvania Sandstone can be used in the analysis. Further, as that portion of the Sylvania Sandstone (lower portion) responds to the general downwarp an increase in horizontal compressive stress along the upper portion also occurs. Thus combination of the reduction of the upper plate or beam to unconfined conditions, the high in situ horizontal stress (nearly the unconfined compressive strength of the low-strength Sylvania), and an increase in horizontal stress with downwarp bring the upper portion of the sandstone beam or plate toward failure.

The bedding character of the Sylvania Sandstone varies regionally. Examination of cores indicates the Sylvania is massive throughout its entire thickness at the Point Hennepin brine field. The lower Sylvania, however, is thin bedded with numerous shale and (or) clay partings as observed at the Ottawa Silica Company, Rockwood, Michigan, quarry approximately 15 mi south of Wyandotte, Michigan.

Geometries for analysis consisted of plate and beam thicknesses varying between 10 and 80 ft and lengths varying between 200 and 1,500 ft. This array is consistent with observed bedding variation and areas of influence of general subsidence (Nieto-Pescetto and Hendron, 1977). Although beam and plate models were eventually discarded in favor of a linear arch model, the analysis using the former models is presented because some aspects of it reinforce and make the linear arch model more realistic.

Beam and Plate Theory Model

A beam model was quickly discarded in favor of plate model as the areal extent of general subsidence and sink formation reflect a three dimensionality of the stress field of the mechanism of subsidence which could not be handled by beam theory. It is worth noting when both simply supported and clamped end beam geometry approached square plate geometry it was found that for self-weight conditions, plate theory predicted approximately one-half the center deflection as compared to beam theory, while the compressive fiber stresses were double those calculated using beam theory. The only difference is two simply supported or clamped ends for the beam, versus four sides simply supported or clamped for the plate. This observation was used in later analysis in extending linear arch theory to a three-dimensional linear arch theory as a first order approximation. For sample calculations see Appendix A.

Various plate geometries, that is, rectangular, square, circular, were considered initially but greater effort was oriented toward circular plate theory as this geometry more closely reflected the actual three-dimensional conditions observed in the field. A typical circular plate schematic diagram is shown in figure 17 where the plate is simply and uniformly supported along the circumference and is loaded by a effective self weight of 100 lb/ft^3. This effective weight was consistently used in the analysis for the Sylvania. A simply supported plate model was used as the low tensile strength of the rock would preclude the development of clamped ends and the simple support yielded more greater values of deflection. A constraint in vertical deflection of 7 ft was introduced. This was done because larger deflection values would not be consistent with observed rock-surface vertical displacements (subsidence measurements) and with the dimensions of the opening observed in experimental bore hole X-5 (D. J. Dowhan, written commun., 1976). With the constraint on allowable deflection the generated stresses were of lower values, so the simple supported plate theory is more conservative with respect to stress generation than clamped end theory.

Figure 18 is a plot of maximum horizontal compressive stress developed as a function of plate thickness for various plate widths. Also shown are the maximum and minimum unconfined compressive strengths of the Sylvania Sandstone as previously discussed, and the stress generated at a maximum allowable deflection of 7 ft. Sample calculations are shown in Appendix B. The constraint of a maximum allowable deflection of 7 ft dramatically limits the quantity of Sylvania Sandstone that can fail, that is, only the sandstone of compressive strength less than approximately 3,000 psi can fail. Examination of figures 15 and 18 reveals that approximately 20 percent or 15 ft of the Sylvania will thus fail compressively and will be reduced to granular sand. The in situ horizontal stresses are not added in figure 18. Adding the in situ horizontal stresses would increase the failure envelope, but not to the extent required for the proposed hypothesis.

Plate theory presents an overly conservative (low) conception of the quantity of sandstone that will fail compressively and thus be reduced to granular sand. The reason being that a tensile field of equal magnitude to the compressive field is assumed to occur. This field acts opposite to the compressive field and in effect reduces the deflection of the plate and thus the fiber stress. In reality, as the tensile strength of rock is approximately 5 percent the compressive strength and the rock is jointed, there is no reason to believe the tensile field will assist in reducing deflection of the compressive stresses on the upper fiber. As indicated before, the result is that less than 20 percent of the sandstone will fail compressively. The conceptual model presented here, however, requires that an appreciable percentage of sandstone fails compressively and be reduced to granular sand.

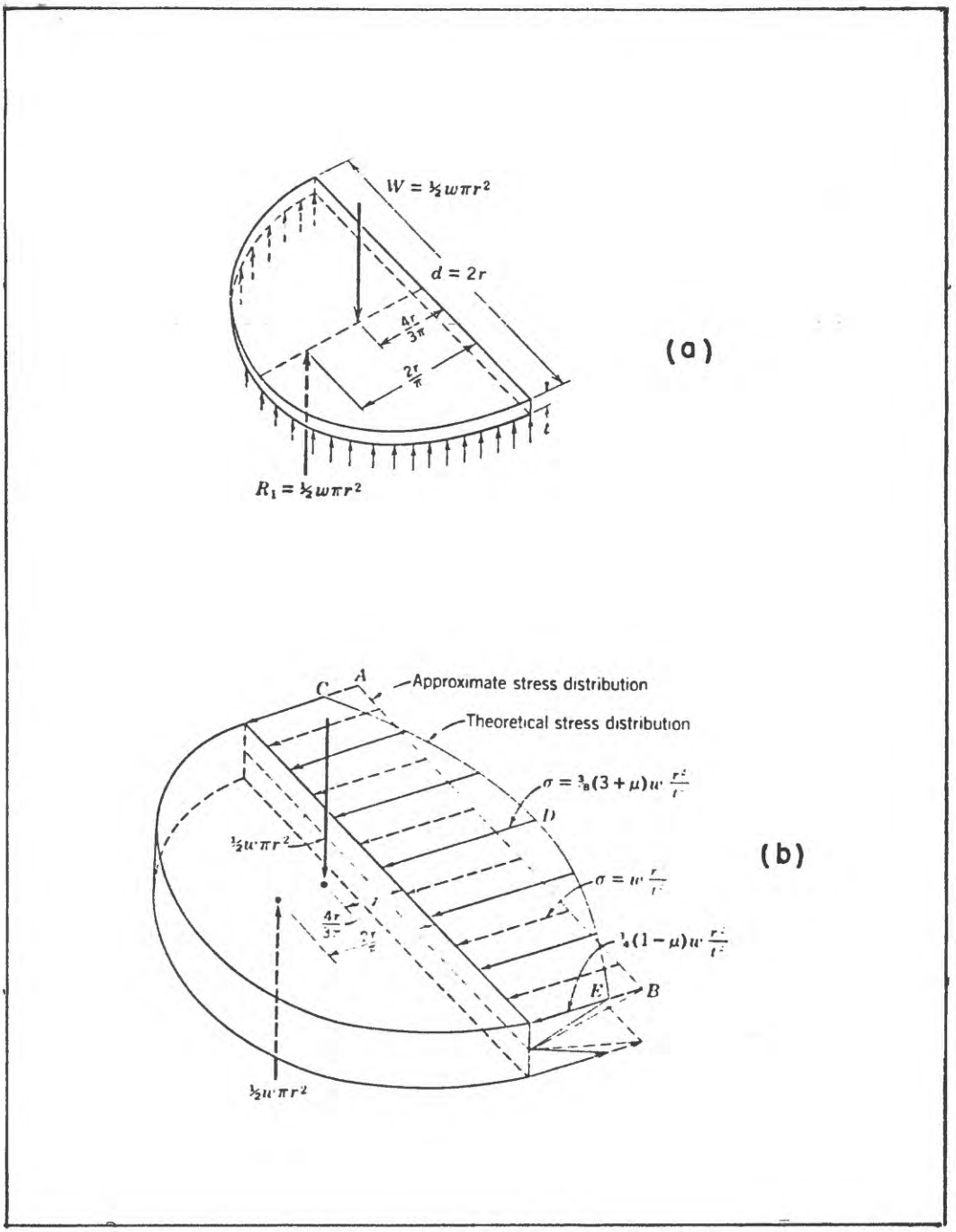

Figure 17.--Diagrams showing a) forces acting on a flat circular plate, uniformly supported and loaded by self weight and b) the stresses developed in the circular plate under uniform load (after Seely and Smith, 1952).

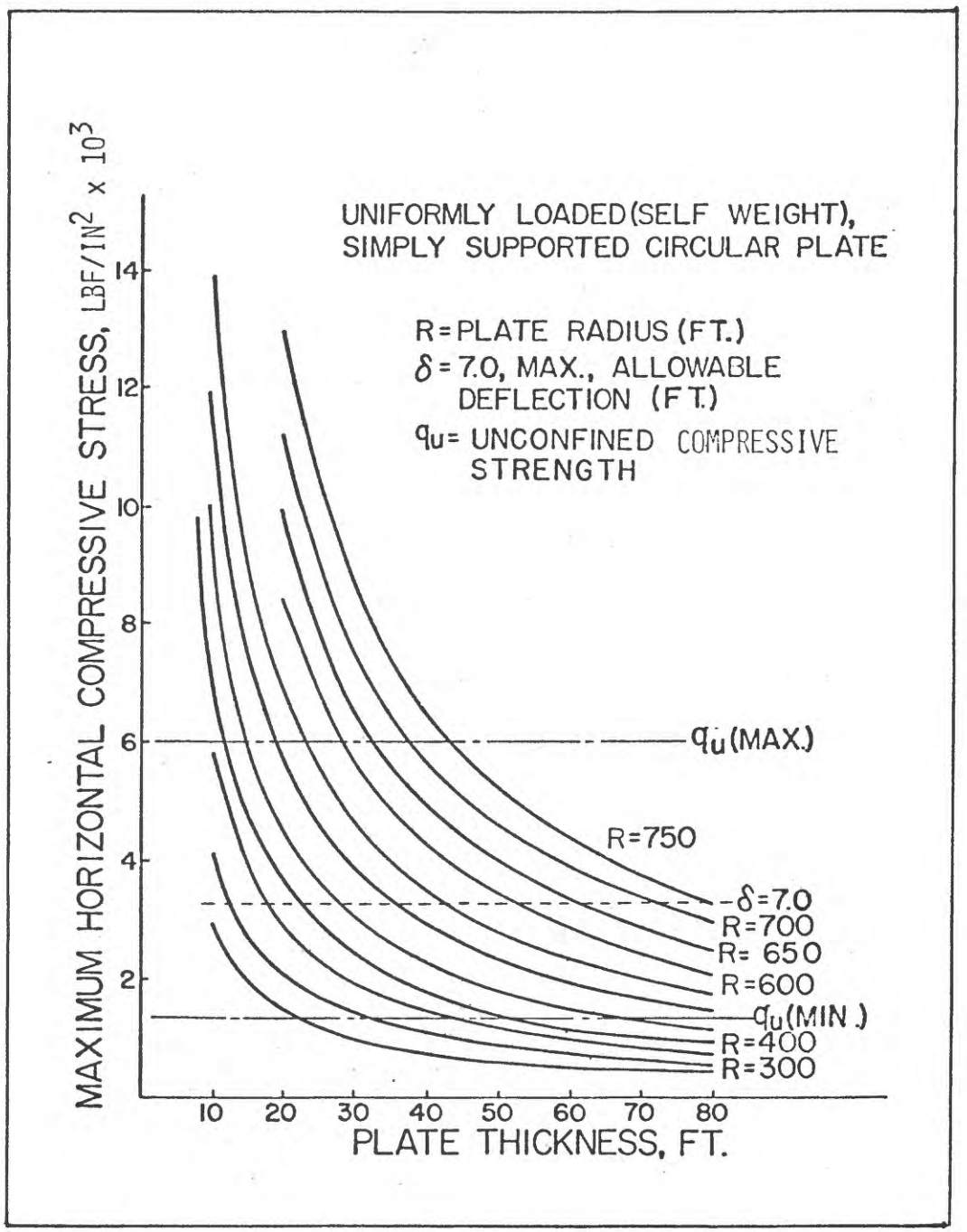

Figure 18.--Set of curves of various radii for plate geometries showing maximum horizontal compressive strength (ordinate) versus plate thickness (abscissa).

Due to the deficiencies discussed above, both beam and plate theories were abandoned in favor of analyzing the Sylvania Sandstone in terms of linear arch theory (Woodruff, 1966, Sterling, 1977).

Linear Arch Theory Model

The theory of voussoir arches has long been known to the civil engineering profession and has been used in construction as a mode of self support in homogeneous jointed beams or plates. The arching action of a jointed or fractured roof rock, overlying a cavity, was demonstrated both rheoretically and experimentally (Evans, 1941) as a practical mode of analysis of unsupported roof rock.

The stability of a linear arch is a function of its thickness to length ratio as well as the modules of elasticity and strength of the rock. The modulus of elasticity directly effects the amount of yield along the arch line which in turn determines the sag or vertical deflection of the linear arch.

Linear arch theory predicts two modes of failure of interest to this investigation: (1) arch crushing, a compressive failure of the upper portion of the arch due to the vertical deflection of the arch induces compressive stresses exceeding the compressive strength of the arch, and (2) arch collapse, where the vertical deflection of the beds creates strains along the arch line which reduces the arch line to a length less that the original arch length (Woodruff, 1966).

An array of arch geometries, similar to that investigated using circular plate theory, was established to include both massive and thin-bedded Sylvania Sandstone of arch lengths from 200 to 1,000 ft. The array was investigated for both the arch-crushing and arch-collapse mode. Envelopes representing each failure mode for various arch geometries were established. Figure 20 is the result of the parametric study for a two-dimensional arch model and shows a plot of maximum horizontal compressive stress developed as a function of arch thickness. Also shown are the maximum and minimum unconfined compressive strengths of the Sylvania Sandstone. Included in this plot also are zones I and II. Zone I represents the arch-collapse mode; zone II the arch crushing mode (for sample calculations see Appendix C). The dot-dashed line separating zones I and II represents the condition where the total shortening of the arch line due to accumulated strain in the arch and abutment is such that is equal to the original arch length.

Thin arches (thin-bedded sandstone) would normally undergo arch collapse while thick arches (more massively bedded sandstone) would normally undergo arch crushing.

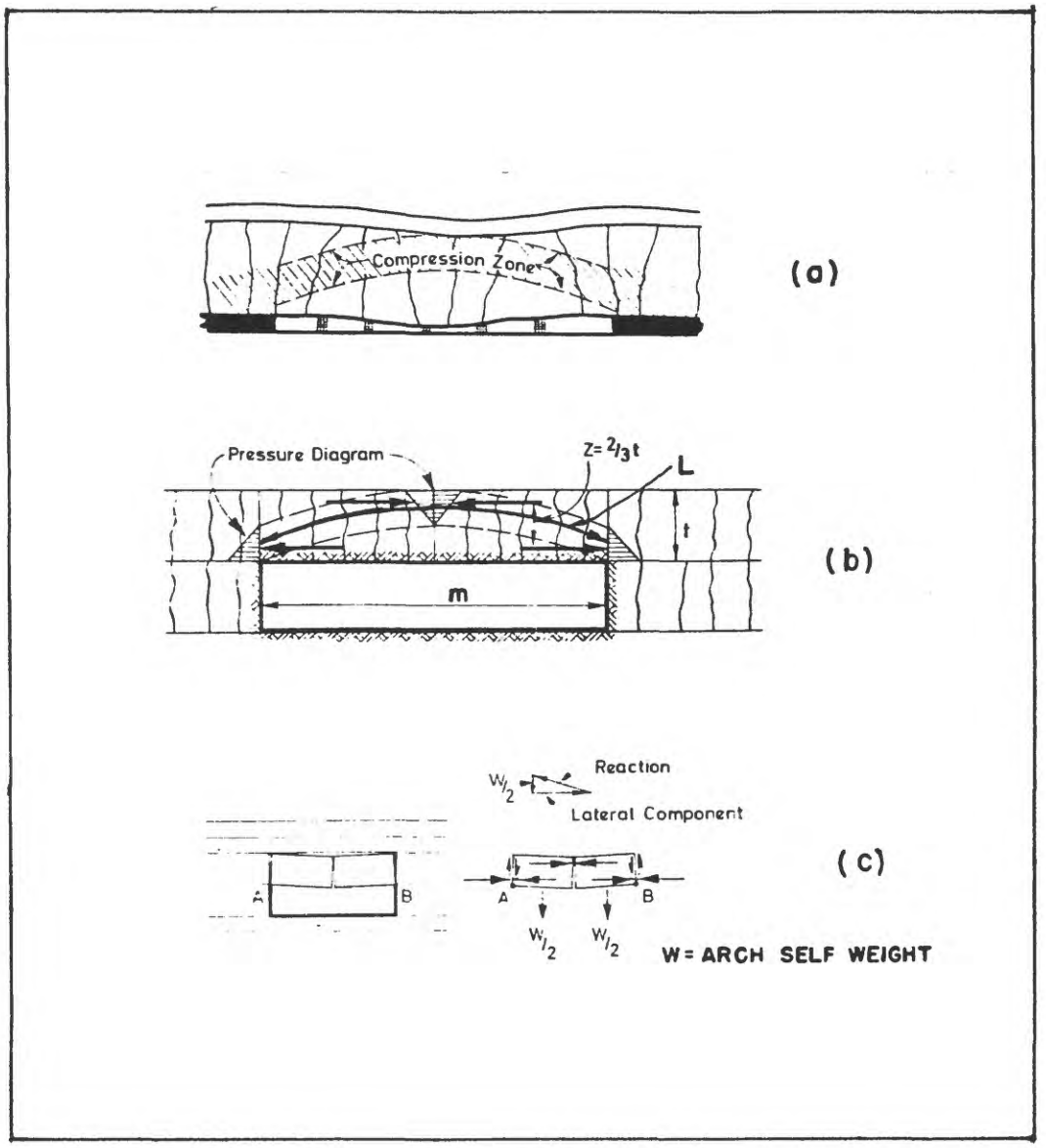

Figure 19.--Diagrams of a) compressive zone within a deflecting linear arch overlying an open cavity, b) the compressive pressure fields developed in linear arch with elements shown, and c) arching action for jointed rock where arch reactions are transmitted through series of minor arch systems (after Woodruff, 1966).

Zone II of figure 20 represents, then, the selection of arch geometries which when loaded by self weight due to sagging underlying dolomite would fail compressively, with the resulting formation of loose granular sand. The sandstone that could fail by the desired compressive failure, zone II, represents an appreciable portion of the compressive strength envelope (up to nearly 6,200 psi) of the Sylvania Sandstone (fig. 20) found at the Point Hennepin brine fields. Approximately 65 ft of the Sylvania could be reduced to sand. Since, as previously mentioned, core examinations and core description (Horvath, 1957) revealed the Sylvania Sandstone to be more massively bedded in the Point Hennepin area one would expect to experience the compressive type failure with the resulting loose granular sand, and eventual sink development.

It must be emphasized, however, that figure 20 represents a two-dimensional arch with abutment reactions at only two ends of the arch. In our case the Sylvania Sandstone must be considered three dimensional plate with reactions at four ends. Further, the in situ horizontal stresses are not added. Thus one would easily expect that there appears to be more than adequate horizontal stresses to induce the compressive failure of the Sylvania Sandstone.

Three-Dimensional Linear Arch Model

As previously mentioned, a first order approximation of a three-dimensional arch can be made by using the same analogy as was used when considering the beam and plate theory for similar geometry (see Appendix D for calculations).

Figure 21 shows the results of a parametric study for three-dimensional arch using the modified form of Woodruff's (1966) linear arch theory (Appendix D) to analyze parametrically the identical array of arch geometries. Figure 21 is a plot of maximum horizontal compressive stress developed as a function of arch thickness for various arch widths. Included are the maximum and minimum unconfined compressive strengths of the Sylvania Sandstone. Also shown in this plot are the two zones discussed previously. Zone I represents the arch-collapse mode and zone II the arch-crushing mode. Figure 21 is similar to figure 20 but the diagonal representing the boundary of arch-collapse and arch-crushing mode of failure is somewhat steeper.

For the three-dimensional linear arch, then, the arch-collapse zone (zone I) is smaller than that for the two-dimensional linear arch (fig. 20) and consequently the three-dimensional linear arch-crushing zone is larger. However, the sandstone beds, being massive (more than 50 ft) at Point Hennepin, cause compressive failure of material with compressive strengths up to nearly 6,000 psi. Considering figures 15 and 21, this represents compressive failure of an appreciable portion of the Sylvania Sandstone, approximately 95 percent or 80 ft.

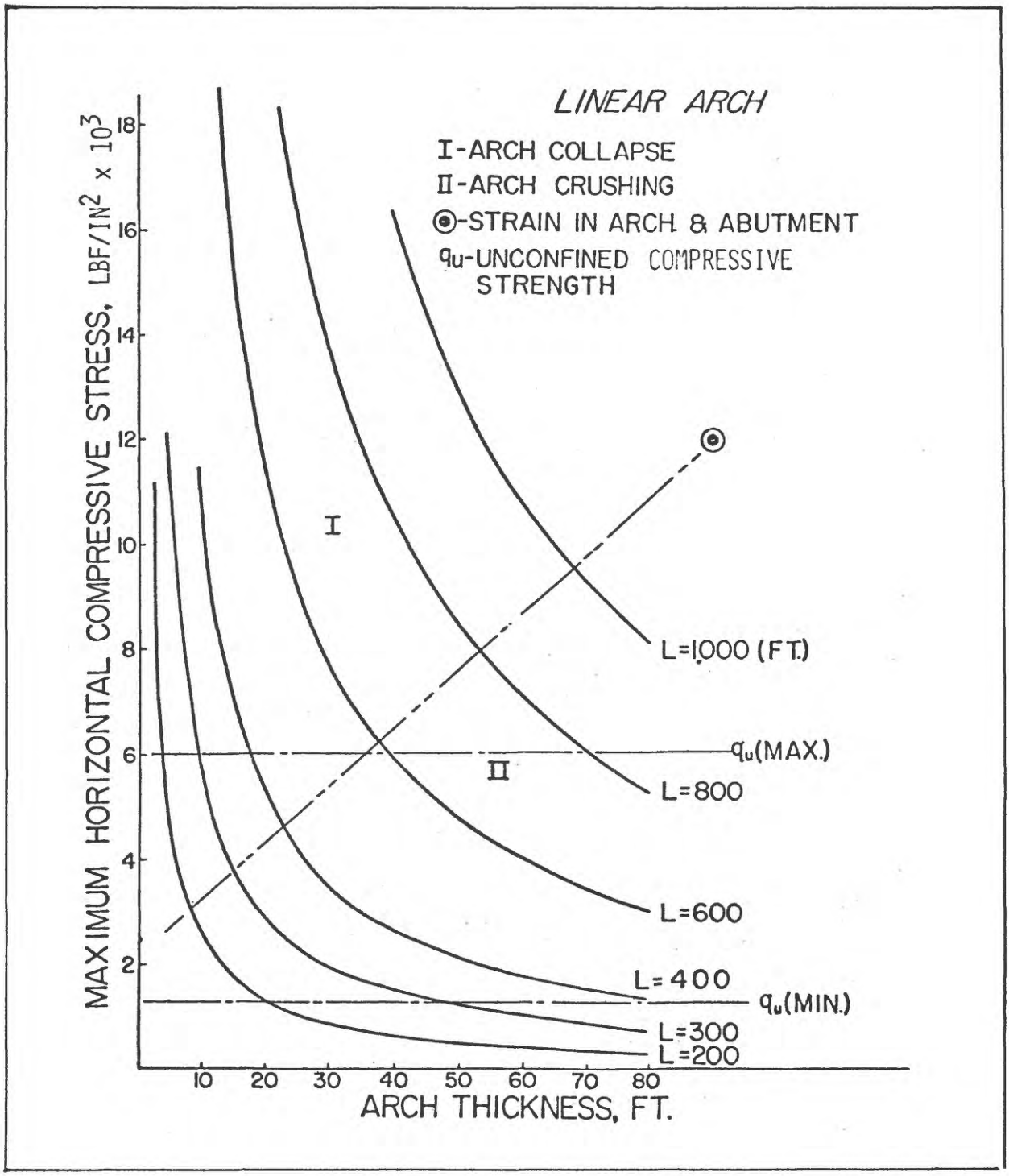

Figure 20.--Set of curves for various length and thickness of linear arches with maximum horizontal compressive strength (ordinate) and arch thickness (abscissa) showing zone of arch collapse and zone of arch crushing with minimum and maximum measured uniaxial compressive strengths for dry samples tested.

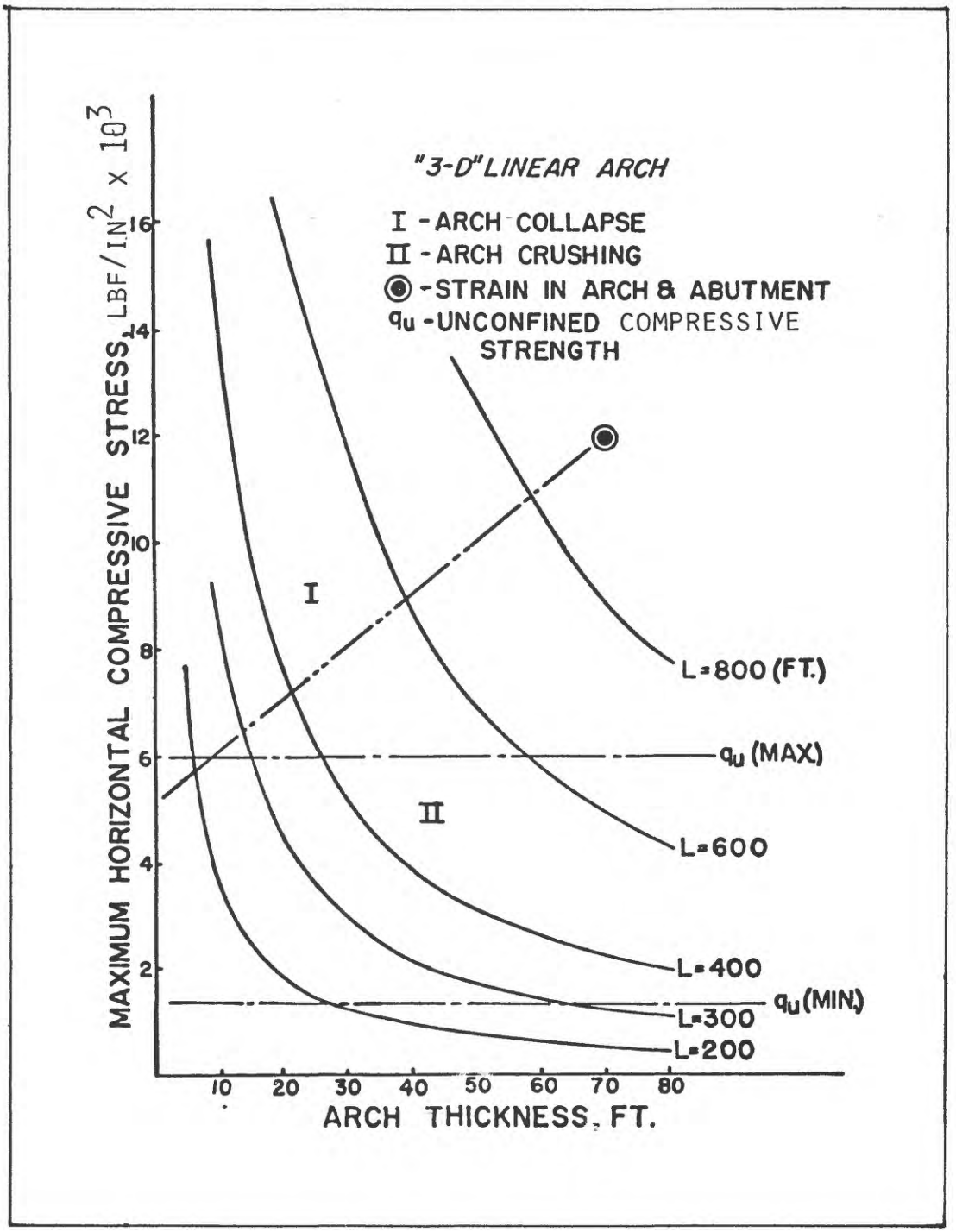

Figure 21.--Set of curves for various lengths and thicknesses of "3-D" linear arches with maximum horizontal compressive strength (ordinate) and arch thickness (abscissa) showing zones of arch collapse and arch crushing with minimum and maximum measured uniaxial compressive strength for dry samples tested.

Figures 22-25 show a conceptualization of the sequence of events leading to the shallow origin of the Detroit area sinks.

Figure 22 shows the result of stoping of brine cavity roof rock and the resulting general subsidence. The sagging of the Sylvania Sandstone, under a high initial in situ horizontal stress field causes separation along the weak zone. The lower Sylvania Sandstone follows the lower dolomite and the upper Sylvania Sandstone adheres to the overlying dolomite. Increased sagging induces higher horizontal stresses resulting in failure of more and more of the lower strength Sylvania Sandstone, and causes the gap within the Sylvania Sandstone to increase in areal extent. Below the Sylvania Sandstone, the formerly tight joint sets open, providing paths for sand-slurry migration to lower depths. Figure 23 shows the results of increased sag causing higher horizontal stress fields which cause a greater portion of the Sylvania Sandstone to fail with the areal extent of the cavity increasing as well. Eventually the areal extent of the cavity reaches a point where the weight of the overlying dolomite and clay cannot be supported and a typical parabolic failure of the roof occurs (fig. 24)

The roof failure above the Sylvania Sandstone allows a path for migration of the 80-100 ft of clay vertically downward, with the filling of the remaining cavity within the Sylvania Sandstone and the Detroit River Dolomite. The surface expression is a sink. Figure 25 shows the final step of sink development where the sink increases in areal extent due to instability of the walls and decreases in depth as the wall material collapses into the sink.

Due to the highly jointed and fractured nature of the Detroit River Dolomite and the unconsolidated clay overlying the Sylvania Sandstone, a parabolic slump failure of these materials is expected. In figure 26, a similar parabolic slump structure is shown in glacial outwash where a slump block, approximately 4 ft wide and 5 ft high, formed when a buried ice block melted out.

In addressing the question of why sinks are found at Point Hennepin and Windsor brine fields and not at the brine fields under the BASF North and South Works, it seems logical to assume the horizontal stress field never developed at the latter sites to a sufficient extent to cause compressive failure of a large portion of the Sylvania Sandstone. Nieto-Pescetto and Hendron (1977) determined the surface gradients just prior to sink development of the subsidence bowls at the North and Central galleries, at Point Hennepin, and at Windsor. The gradients were found to be 2.47 in./100 ft, 2.39 in./ft, and 2.75 in./100 ft, respectively, whereas surface gradients at the North Works at Wyandotte prior to suspension of solution mining was only 1.8 in./100 ft.

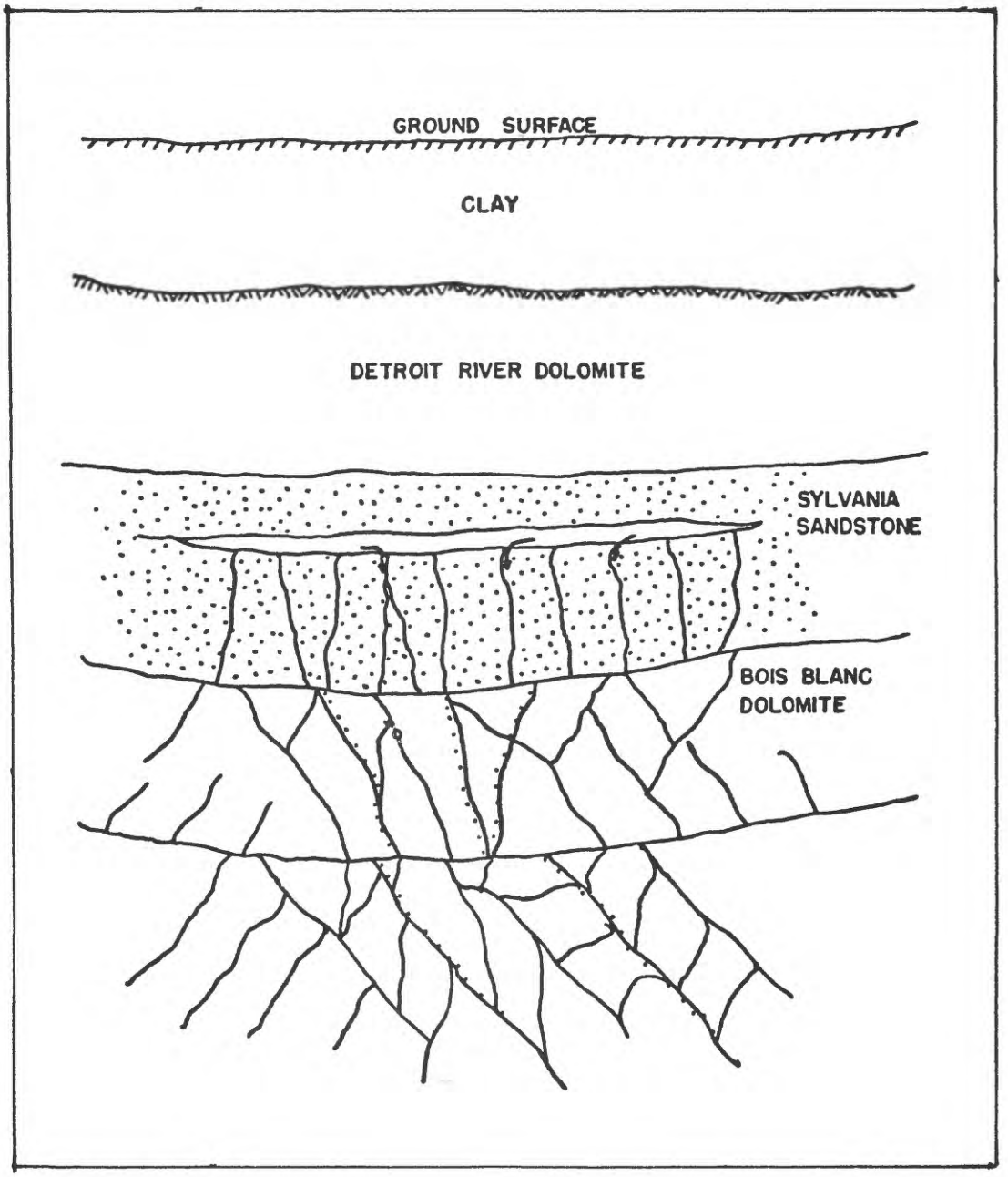

Figure 22.--Sketch showing initial sagging of Sylvania Sandstone as responding to sagging of lower dolomite with separation of weak zone.

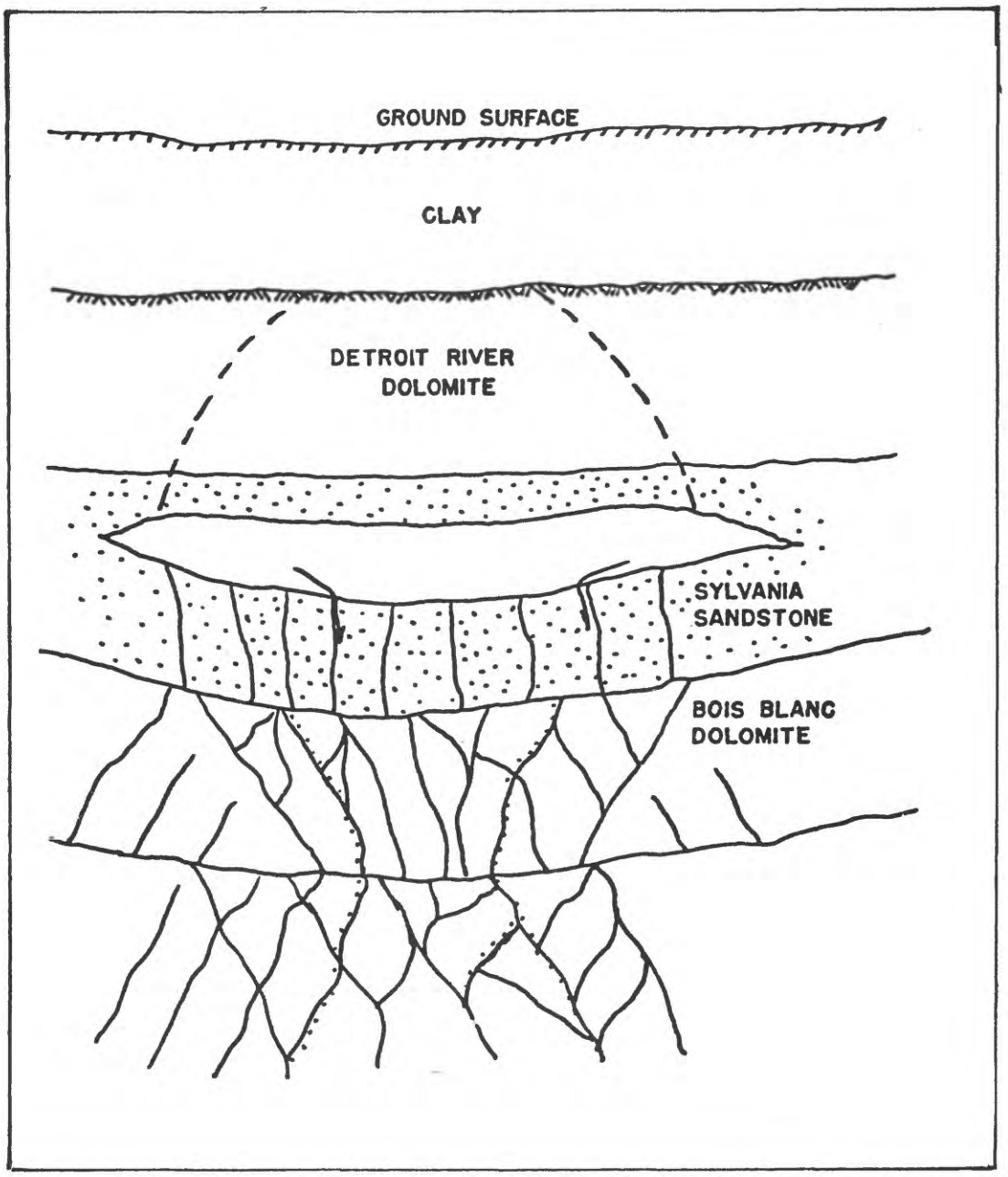

Figure 23.--Sketch showing increased sagging of Sylvania Sandstone with greater crushing of weaker Sylvania Sandstone and migration of loose sand vertically downward. Incipient failure of roof of cavity within Sylvania Sandstone.

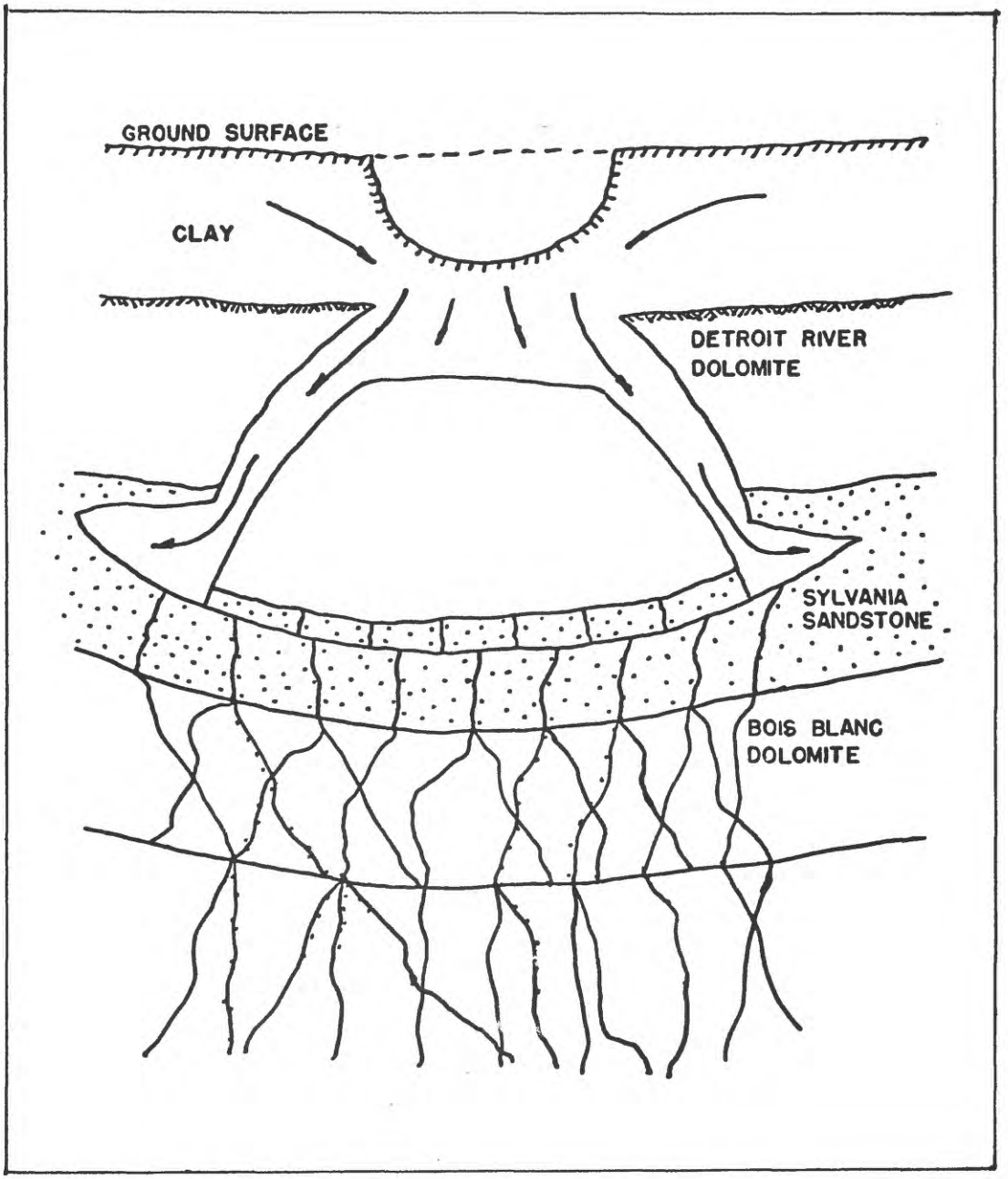

Figure 24.--Sketch showing failure of the overlying highly jointed and fractured dolomite and development of a sink at the surface with unconsolidated clay flowing into the voids.

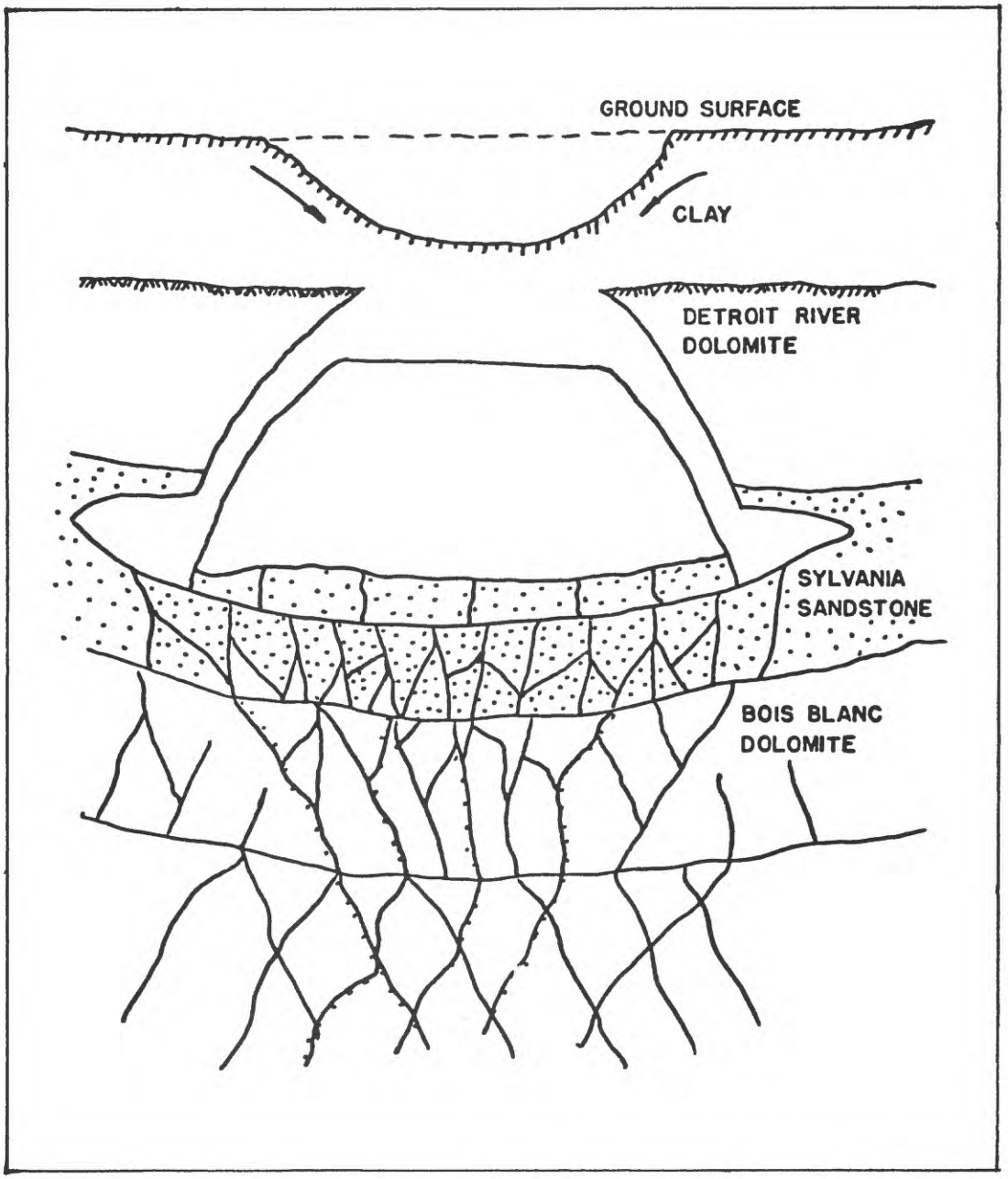

Figure 25.--Sketch showing final phase of the sink episode with the effects of weathering reducing depth of sink with material removed from walls.

Figure 26.--Photograph showing a typical parabolic clump in unconsolidated glacial outwash overlying a melted out ice block (modified from McDonald and Shilts, 1975).

The surface gradients (rate of settlement derived by precise leveling surveys) are subdued indicators of vertical deflections or sagging measured at the surface, presumably also occurring on the Sylvania Sandstone. The sag is proportional to increases in horizontal stress. Above the North and South galleries the increase in horizontal stress, as reflected by the surface gradients, was insufficient to cause extensive compressive failure of the Sylvania Sandstone as is theorized to have occurred at Point Hennepin.

Sinks can be expected only where the Sylvania is massively or thickly bedded and cannot be predicted to occur everywhere the Sylvania is found. The Sylvania sand can migrate vertically downward forming a shallow cavity with subsequent sink development fairly rapidly (in as short a time as a week). This compares to the years required for brine well coalescence and eventual downwarp of the overlying roof rock.

CONCLUSION

The hypothesis of a shallow origin of the Detroit area sink rests on a combination of unique features:

- Compressive strengths of critical portions of the Sylvania Sandstone very nearly equal the in situ horizontal stress present in the area.

- The highly dilatant behavior and explosive compressive failure of the Sylvania Sandstone upon loading.

- The induction of additional horizontal stresses with general subsidence.

- The extensive joint system that permeates rock units and provides many paths for the fine-grained loose sand to migrate vertically downward.

Further, the hypothesis of a shallow origin of sinks is supported by cases of coal extraction at various depths with a variety of subsurface lithologies. Hunt (1980) has shown that sinks form only when the coal measures were extracted from depths less than 200 ft from the ground surface. Deeper extractions result in sags (general subsidence) only.

RECOMMENDATIONS

Further investigations are recommended to substantiate the shallow depth hypothesis of sink formation presented in this study.

Exploratory core holes in the vicinity of experimental hole X-5 and within existing sinks are recommended to determine if the depth and areal extent of the cavity within the Sylvania Sandstone is increasing in the area of experimental hole X-5. A determination should be made to verify that the displacements of the Detroit River Dolomite and clay as proposed by this hypothesis have occurred over existing sinks.

Precise levelling measurements in the area of experimental hole X-5 and the existing sinks might provide valuable insight into subsurface movement.

Core holes drilled in the former mainland brine field in the nearby North Works are suggested to provide samples and access to the Sylvania Sandstone for determination of physical properties and geologic details in order to answer the question as to the lack of sinks in this field even though larger quantities of salt were extracted than at the Point Hennepin brine field.

A determination of the in situ horizontal stress field (Franklin and Hungr, 1978) with depth in the Detroit area would be of considerable benefit in the understanding the exact horizontal stress field within the Sylvania Sandstone as it affects the proposed failure mechanism.

REFERENCES

Boretti-Onyszkiewicz, W., 1966, Joints in the Flysch Sandstones on the ground of strength examinations: Congress of International Society of Rock Mechanics, 1st, Lisbon, Proceedings, v. 1, p. 153-157.

Bottoms, K. P., 1959, A study of the Middle Devonian strata of the southern peninsula of Michigan based on a well core from Grosse Ile, Michigan: Ann Arbor, University of Michigan Masters thesis, p. 10-15.

Carman, J. E., 1936, Sylvania Sandstone of northwest Ohio: Geological Society of America Bulletin, v. 47, p. 253-266.

Dorr, J. A., Jr., and Eschman, D. F., 1970, Geology of Michigan: Ann Arbor, University of Michigan Press, p. 113-123.

Dowhan, D. J., 1976, Test drilling to investigate subsidence in bedded salt: BASF Wyandotte Corporation, Wyandotte, Michigan, p. 1-13.

Ege, J. R., 1979a, Selected bibliography on ground subsidence caused by dissolution and removal of salt and other soluble evaporites: U.S. Geological Survey Open-File Report 79-1133, 28 p.

_____1979b, Selected bibliography on subsidence processes and related engineering problems in carbonate rocks: U.S. Geological Survey Open-File Report 79-1214, 24 p.

_____1979c, Surface subsidence and collapse in relation to extraction of salt and other soluble evaporites: U.S. Geological Survey Open-File Report 79-1666, 34 p.

Evans, W. H., 1941, The strength of undermined strata: Institution of Mining and Metallurgy Transactions, 1940-1941, p. 475-500.

Franklin, J. A., and Hungr, O., 1978, Rock stresses in Canada, their relevance to engineering projects: Rock mechanics, supp. 6, p. 25-46.

Grabau, A. W., and Sherzer, W. H., 1910, The Monroe Formation of southern Michigan and the adjoining regions: Michigan Geological Survey, Publication 2, Geological Series I, p. 61-86.

Herget. G., 1973, Variations of rock stresses with depth at a Canadian iron mine: International Journal of Rock Mechanics and Mining Science, v. 10, p. 37-51.

Herget, G., Pahl, A., and Olive, P., 1975, Ground stresses below 3,000 feet: 10th Canadian Rock Mechanics Symposium, Kingston, Ontario, Proceedings, p. 281-307.

Horvath, A. L., 1957, The stratigraphy and paleontology of drill hole H-1A, Taylor Township, Wayne County, Michigan: Ann Arbor, University of Michigan Masters thesis, 33 p.

Hunt, S. R., 1980, Surface subsidence due to coal mining in Illinois: Urbana, University of Illinois Ph. D. thesis, 125 p.

Kalafatis, C. A., 1958, The stratigraphy and paleontology of core H-1A of Upper Silurian strata, from Taylor Township, Wayne County, Michigan: Ann Arbor, University of Michigan Masters thesis, p. 1-45.

Landes, K. K., 1945, The Salina and Bass Islands rocks of the Michigan Basin: U.S. Geological Survey Oil and Gas Investigations Preliminary Map OC-40.

_____1949, Detroit River Group in the Michigan Basin: U.S. Geological Survey Circular 127, p. 1-23.
_____1951, Detroit River Group in the Michigan Basin: U.S. Geological Survey Circular 133, p. 1-23.
_____1963, Effects of solution of bedrock salt on the Earth's crust, in Bersticker, A. C., ed., Symposium on Salt, 1st, Cleveland, 1962 Proceedings: Northern Ohio Geological Society, p. 64-73.
Landes, K. K., and Piper, T. B., 1972, Effect upon environment of brine cavity subsidence at Grosse Ile, Michigan: Solution Mining Research Institute and BASF Wyandotte Corporation, p. 10.
Lockett, J. R., 1947, Development of structures in basin areas in northeastern United States: American Association of Petroleum Geologists Bulletin, v. 31, p. 429-446.
McDonald, B. C., and Shilts, W. W., 1975, Faults in glacifluvial sediments, in Jopling, A. V., and McDonald, B. C., eds., Glaciofluvial and glaciolacustrine sedimentation: Society of Economic Paleontologists and Mineralogists Special Publication 23, p. 123-131.
Newcombe, R. B., 1933, Oil and gas fields of Michigan: Michigan Geological Survey Publication 38, 293 p.
Nieto-Pescetto, A. S., 1974, Experimental study of the shear-stress behavior of clay seams in rock masses: Urbana, University of Illinois Ph. D. thesis, 207 p.
Nieto-Pescetto, A. S., and Hendron, A. J., Jr., 1977, Study of sink-holes related to salt production in the area of Detroit, Michigan: Solution Mining Research Institute, Inc., p. 1-50.
Pirtle, G. W., 1932, Michigan structural basin and its relationship to surrounding areas: American Association of Petroleum Geologists Bulletin, v. 16, p. 145-152.
Querio, C. W., 1977, Current practices in solution mining of salt, in Martinez, J. D., and Thoms, R. L., eds., Symposium on Salt Dome Utilization and Environmental Considerations, Baton Rouge, 1976 Proceedings: Institute for Environmental Studies, Louisiana State University, p. 3-41.
Reavely, G. H., and Winder, C. G., 1961, The Sylvania Sandstone in southwestern Ontario: Canadian Mining and Metallurgical Bulletin, v. 64, p. 109-112.
Sanford, B. V., and Brady, W. B., 1955, Paleozoic geology of the Windsor-Sarnia area, Ontario: Canada Geological Survey Memoir 278, p. 1-65.
Savage, W. Z., 1979, Prediction of vertical displacements in a subsiding elastic layer--a model for subsidence in karst terrains: U.S. Geological Survey Open-File Report 79-1094, 13 p.
Seely, F. B., and Smith, J. O., 1952, Advanced mechanics of materials: New York, John Wiley, p. 220-230.
Sherzer, W. H., and Grabau, A. W., 1909, The Sylvania Sandstone--Its distribution, nature and origin: Michigan Geological Survey, p. 61-86.
Smith, R. A., 1937, Some new aspects of the Michigan Basin [abs.]: Geological Society of America Proceedings, p. 326.

Sterling, R. L., 1977, Roof design for underground openings in near-surface bedded rock formations: University of Minnesota Masters thesis, p. 57-128.

Woodruff, S. D., 1966, Methods of working coal and metal mines, V. 1: New York, Pergamon Press, 538 p.

APPENDIX A

Square Plate Simply Supported at Two Ends

To calculate the stress developed in a square plate, simply supported at two ends, and loaded by self weight using beam theory, consider a square plate of dimensions 400 ft on each side and 60 ft thick. The effective unit-weight (w) is 100 lb/ft^3.

The total magnitude of the load on the square plate is

$$W = w(400)^2(60) = 9.6 \times 10^8 \text{ lb.}$$

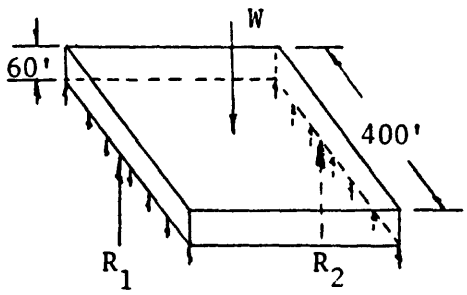

The resultant reactions at each of the supported ends of the plate are:

$$R_{1,2} = W/2 = 4.8 \times 10^9 \text{ lb.}$$

The greatest bending stress will occur at the center of the square plate. Considering a free body diagram of half the square plate with the left end reaction R_1, the load of the half-plate (W/2) passing through the controid of the half-plate,

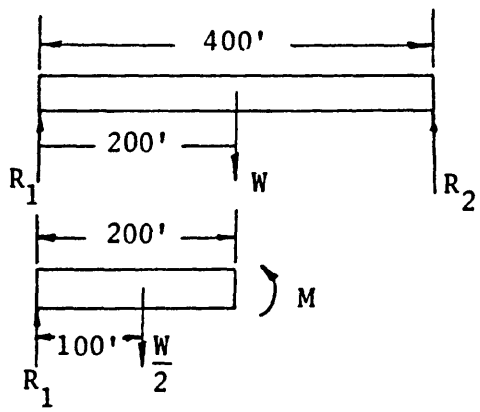

the bending moment is:

$$M = R_1 (200) - \frac{W}{2}(100)$$

$$M = 4.8 \times 10^{10} \text{ lb/ft.}$$

The maximum bending stress due to the bending moment M is:

$$\sigma_{max} = \frac{MC}{I}$$

where C = 30 ft, the distance from the neutral axis of the square plate to its outer (top and bottom) fibers.

$$I = \frac{bh^3}{12} = \frac{1}{12}(400)\ (60)^3 = 7.2 \times 10^6\ ft^4$$

$$\sigma_{max} = 1{,}389 \text{ psi (compression and tension)}$$

Restricting the deflection of the beam theory treatment to that developed using the plate theory analysis requires, then, the calculating of a new equivalent load, w, that will limit deflection for the beam (Seeley and Smith, 1952) for the range of plate geometries considered in the parametric study (p. 64). The ratio of bending stress using plate theory to bending stress using beam theory reached 1.5:1. However, no restriction was made, with the beam analysis, on limiting center deflection. The restriction of center deflection is discussed in appendix B.

APPENDIX B

Circular Plate with the Entire Edge Supported

Because the stresses in the center of a circular plate are nearly equal to the stresses in the center of a square plate of similar geometry, and a circular plate represents more nearly field conditions, the calculations are for a circular plate. To calculate the stress developed within a circular plate, simply supported at the edge, loaded by self-weight, we will define such a plate (fig. 17a, b) of radius, r, of constant thickness, t, and subjected to a uniformly distributed self-weight. The effective unit-weight, w is 100 lb/ft ^{3}.

The bending moment, about any diameter, of the forces lying to one side of a vertical diametrical plane (fig. 17a) is simply the moment of the reactions minus the moment of the load.

The magnitude of the load on the half-plate is:

$$W = \frac{1}{2}\ (\pi r^2 t w)$$

with its action line passing through the centroid of the semicylindrical volume, $4r/3\rho$ from the diametrical plane. The resultant R_1 of the reaction of the supporting rim is equal in magnitude to the self weight with its action line passing through the centroid of the semicircumference, at the distance $2r/\rho$ from the diametrical plane (fig. 17a).

The bending moment, M, about the diameter is:

$$M = R_1\left(\frac{2r}{\pi}\right) - W\left(\frac{4r}{3\pi}\right) = \frac{w\pi r^2 t}{2}\left(\frac{2r}{\pi} - \frac{4r}{3\pi}\right) = \frac{wr^3 t}{3}\ .$$

The bending moment, M, may be equated to the resisting moment at the vertical diametrical section since the moments are in equilibrium.

Assuming the maximum fiber stresses along the vertical diameterical plane are constant (average stress value) and assuming bending in one plane the resisting moment is

$$M = \frac{wr^3t}{3} \text{ and since } \sigma = \frac{MC}{I}, \text{ then}$$

$$M = \frac{wr^3t}{3} = \frac{\sigma_{avg}I}{C}$$

where σ_{avg} is the average bending stress (outer fiber), and where

$$I = \frac{1}{12}(2r)t^3 \text{ and}$$

$$C = \frac{t}{2}.$$

Therefore, $\sigma_{avg} = \frac{wr^2}{t}$ where σ_{avg} is the average maximum bending stress at the surface of the plate at the vertical diametrical section.

The true maximum bending stress due to the parabolic stress distribution, occurs at the center of the plate (fig. 17b) and is

$$\sigma_{max} = \frac{3}{8}(3 + \mu)w'(\frac{r^2}{t^2}) = \frac{3}{8}(3+\mu)w(\frac{r^2}{t})$$

where μ is Poisson's ratio and w' = wt.

The maximum deflection at the center of the plate (δ_{max}) is

$$\delta_{max} = \frac{3}{16}(1 - \mu)(5 + \mu)\frac{w'r^4}{Et^3} = \frac{3}{16}(1-\mu)\frac{wr^4}{Et^2}$$

where E = Young's modulus,
μ = Poisson's ratio and
w' = wt.

APPENDIX C

Linear arch theory considers only the compressive stress field zone (fig. 19a) deflection of a rock mass. The elements of the linear arch are shown in figure 19b with the compressive pressure fields identified and the geometry of a linear arch overlying a rectangular cavity. In highly fractured or jointed rock a combination of a multitude of small arch systems (fig. 19c) will allow the theory to span jointed rock.

Assuming the thickness (t) of the linear arch to be 80 ft, the compressive strength (Q) of the arch material to be 2,400 psi and a modulus of elasticity (E) of 10^6 psi the maximum length of arch (maximum span) for a self-supported, gravity loaded arch is

$$m = 1.24\ (Qt)^{1/2}$$

where Q is in psi
t is in feet
m is in feet.

For the above case m = 543 ft (Woodruff, 1966). The initial height of the line is

$$z_o = \frac{2}{3}t = 53.33 \text{ ft} \qquad \text{(fig. 19b)}$$

The length of the arch line is

$$L = m + \frac{8z_o}{3m} = 557.3 \text{ ft} \qquad \text{(Woodruff, 1966)}$$

The unit elastic strain along the arch line is

$$e_{arch} = \frac{11}{24}\left(\frac{Q}{E}\right) = 0.0011$$

The total strain along arch line is

$$\Delta_{arch}\ Le = 0.613 \text{ ft}$$

The final length of the arch line is

$$L_1 = L\ \Delta_{arch} = 556.69 \text{ ft}$$

which is greater than the maximum possible arch length (m = 543 ft) so the arch is stable to turning inside out (buckling). Of course since the compressive stress of 2,400 psi is mobilized any material of compressive strengths less than 2,400 psi will fail due to crushing.

The following examples further delineate the zones of buckling versus crushing failure using linear arch theory.

Consider first an example of buckling failure.

$t = 10$ ft

$Q = 5{,}000$ psi

$E = 10^6$ psi

$m = 1.24(Qt)^{1/2} = 277.27$ feet, the maximum length of arch

$z = \frac{2}{3t} = 6.67$ ft, the initial height of arch line

$L = m + \frac{8z^2}{31} = 277.698$ ft, the length of the arch line

$e_{arch} = \frac{11}{24}\frac{Q}{E} = 0.00229$, the unit strain along arch line

$\Delta_{arch} = Le = 0.636$ ft, the total strain along the arch

$L - \Delta_{arch} = 277.06$ ft, so the total strain line along the arch line would reduce the arch line length (L) to less than the span of the arch (m) and the arch would simply collapse (buckle) without mobilization of full compressive stress field.

Consider now an example of crushing failure where

$t = 50$ ft

$Q = 5{,}000$ psi

$E = 10^6$ psi

$m = 1.24(Qt)^{1/2} = 620.0$ ft

$z + 33.3$ ft

$L = 624.78$ ft

$w_{arch} = 0.00229$

$\Delta_{arch} = Le = 1.4318$ ft

$\Delta_{abutment} = 0.3125$ ft

The total strain is the sum of the arch line strain and the strain that exists within the abutments themselves. The abutment strain is generally 1/4-1/3 the arch line strain for the series of geometries considered.

$$\Delta_{total} = \Delta_{arch} + \Delta_{abutment} = 1.74 \text{ ft}$$

The revised arch line length is

$$L_i = L - \Delta_{total} = 623.04 \text{ ft}$$

Since $L_i > m$ the arch will not buckle and the entire, 5,000 psi compressive stress field will be developed with weaker material failing by crushing.

APPENDIX D

The extension of linear-arch theory to a three-dimensional linear-arch system where the 3-D arch is supported on four sides was made due to the fact that the brine cavity roof rock is three dimensional.

Recalling the comparison of beam and rectangular plate theory (p. 35 and appendix A) where, when a square plate was analyzed by plate theory and the resulting deflection imposed on the beam analysis a ratio of bending stress for plate theory versus beam theory was found to be 1.5:1.

As a first approximation, then, the linear arch theory can be expanded to a 3-D arch system such that the bending stress developed would double. Therefore

$m = 1.24\ (Qt)^{1/2}$ becomes $m' = (\frac{Qt}{1.5})^{1/2} = 1.01\ (Qt)^{1/2}$

A comparison of the thickness (t) versus length of arch (m) is shown below for compressive strengths of Q = 2,400 psi as an illustration

where $m = 1.24(Qt)^{1/2}$

$m' = 1.01(Qt)^{1/2}$

Q = 2,400 psi

t (ft)	m (ft)	m' (ft)
10	192	271
20	272	384
30	333	471
40	384	543
50	429	607
60	471	665
70	508	719
80	543	768

With the values of m', then, the same analysis is made for buckling versus crushing as in Appendix C.

FACTORS FOR CONVERTING ENGLISH UNITS TO METRIC

UNITS OF MEASUREMENTS

To convert	Multiply by	To obtain
Feet	3.281	Meters
$Feet^2$	$9.29X10^{-2}$	$Meters^2$
$Feet^3$	$2.832X10^{-2}$	$Meters^3$
Inches	$2.54X10^{1}$	Millimeters
Inches	2.540	Centimeters
$Inches^2$	6.452	$Centimeters^2$
$Inches^3$	$1.639X10^{1}$	$Centimeters^3$
Miles	1.609	Kilometers
$Miles^2$	2.590	$Kilometers^2$
Pounds	$4.536X10^{-1}$	Kilograms
Pounds/foot	1.488	Kilograms/meter
$Pounds/foot^2$	4.882	$Kilograms/meter^2$
$Pounds/foot^3$	$1.602X10^{1}$	$Kilograms/meter^3$
$Pounds/inch^2$	$6.895X10^{-3}$	Megapascals